Structure of the Mediterranean Undercurrent and Mediterranean Water spreading around the southwestern Iberian Peninsula

Amy S. Bower
Department of Physical Oceanography, Woods Hole Oceanographic Institution, Woods Hole, Massachusetts, USA

Nuno Serra and Isabel Ambar
Instituto de Oceanografia, University of Lisbon, Lisbon, Portugal

Received 6 June 2001; revised 4 March 2002; accepted 17 May 2002; published 18 October 2002.

[1] RAFOS float and hydrographic data are analyzed to investigate the pathways, rates, and mechanisms of Mediterranean Water (MW) spreading into the North Atlantic from the Gulf of Cadiz, with an emphasis on processes other than meddies. We find that the transition of the Mediterranean outflow from a density current to an intermediate-depth jet occurs as it enters Portimão Canyon south of Portugal due to rapidly steepening topography and associated turbulent entrainment. This feature was not seen in recent plume model simulations due to their use of smoothed topography. In addition to the traditional lower salinity maximum (or core), a denser, deeper continuous vein of MW was also traceable from Portimão Canyon to Cape St. Vincent. The mean velocity structure of the Mediterranean Undercurrent changes from a ~30-km-wide jet with peak mean westward speed of ~0.2 m s^{-1} along the southern Iberian slope, to a broader, much weaker northward flow with maximum mean speed of only ~0.06 m s^{-1} along the western Iberian slope, due in part to changes in the bottom slope. Lower core MW spread mainly (1) southward into the interior Gulf of Cadiz, (2) northward along the western Iberian slope, and (3) westward into the deep Tagus Abyssal Plain. The average spreading rate was 0.01–0.02 m s^{-1} toward the west–northwest direction. Meddies forming near the slope were found to have an indirect but profound impact on MW spreading, often diverting MW approaching from upstream into the interior. The results are compared to recent hydrography-based studies of MW spreading pathways. *INDEX TERMS:* 4520 Oceanography: Physical: Eddies and mesoscale processes; 4516 Oceanography: Physical: Eastern boundary currents; 4536 Oceanography: Physical: Hydrography; *KEYWORDS:* Mediterranean Water, floats, Meddies, physical oceanography, water masses, hydrography

Citation: Bower, A. S., N. Serra, and I. Ambar, Structure of the Mediterranean Undercurrent and Mediterranean Water spreading around the southwestern Iberian Peninsula, *J. Geophys. Res.*, *107*(C10), 3161, doi:10.1029/2001JC001007, 2002.

1. Introduction

[2] The Mediterranean salt tongue is a well-documented hydrographic feature of the North Atlantic thermocline in the subtropics (for recent descriptions, see *Reid* [1994] and *Lozier et al.* [1995]). It results from the overflow of dense, saline water from the Mediterranean Sea through the Strait of Gibraltar. Due to its higher density compared to the ambient Atlantic waters, the overflow descends from the 300-m deep strait down the continental slope of the eastern Gulf of Cadiz, entraining the overlying, less dense North Atlantic Central Water (NACW). As it descends, the overflow turns toward the north and follows the continental slopes of Spain and Portugal through the Gulf of Cadiz (see Figure 1 for geographic locations). Near 8°W, it approaches neutral buoyancy at about 1000 m, and continues westward as a subsurface, boundary-intensified jet known as the Mediterranean Undercurrent [*Madelain*, 1970; *Zenk*, 1975; *Ambar and Howe*, 1979a, 1979b; *Ochoa and Bray*, 1991; *Baringer and Price*, 1997; *Käse and Zenk*, 1996].

[3] The undercurrent turns northward around Cape St. Vincent, at the southwestern corner of the Iberian Peninsula, and continues northward along the continental slope, but a substantial fraction of MW begins to separate from the boundary and enters the interior North Atlantic [see, e.g., *Zenk and Armi*, 1990]. This latter spreading of Mediterranean Water (MW) away from the western Portuguese slope represents the "virtual" source of MW to the open Atlantic, as is apparent in the large-scale mean salinity distribution [*Käse and Zenk*, 1996]. Northward transport of MW in the undercurrent continues probably as far north as Porcupine Bank (50°N), although its characteristics are substantially diluted due to mixing [*Daniault et al.*, 1994; *Iorga and Lozier*, 1999a].

[4] Ever since the distinctive shape of the Mediterranean salt tongue was recognized, investigators have been trying to understand the processes that spread MW from its source into the ocean interior. Some success in reproducing its general

0148-0227/02/2001JC001007$09.00

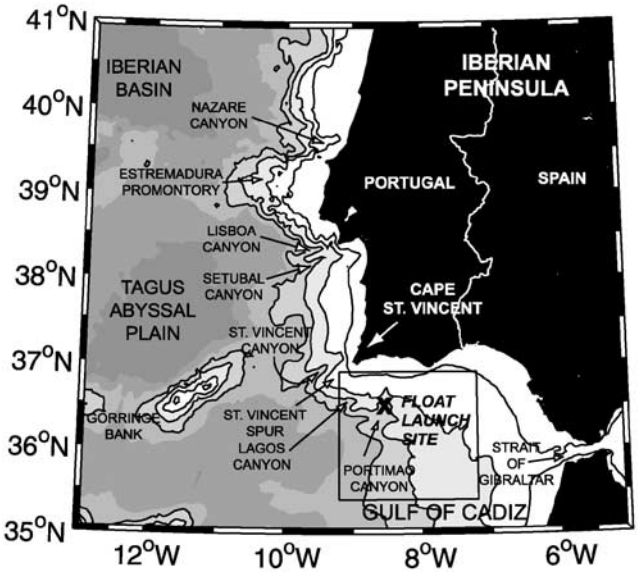

Figure 1. Chart showing bathymetry off the southwestern Iberian Peninsula. Bottom depth is shaded in 1000-m intervals and contoured at 200, 1000, 2000 and 3000 m. The RAFOS floats launched during A Mediterranean Undercurrent Seeding Experiment (AMUSE) were deployed near 36.5°N, 8.5°W (position indicated by the "x"). The box illustrates the area of the hydrographic survey shown in Figure 2.

shape was realized using simple advective–diffusive models [*Needler and Heath*, 1975; *Richardson and Mooney*, 1975] But the discovery of energetic, long-lived, coherent vortices with a core of high-salinity water (called meddies), first in the western North Atlantic [*McDowell and Rossby*, 1978], and then in the eastern Atlantic [*Armi and Zenk*, 1984], challenged the traditional view of MW spreading processes. In the past 20 years, many meddies have been observed, their structure and life histories documented (for reviews, see *Bower et al.* [1997a] and *Richardson et al.* [2000]). Estimates of meddies' contribution to the westward salt flux range from 25% [*Richardson et al.*, 1989] to nearly 100% (includes meddies and other eddies [*Mazé et al.*, 1997]).

[5] In 1993–1994, we seeded the Mediterranean Undercurrent south of Portugal with acoustically tracked RAFOS floats and tracked them for up to 11 months [*Hunt et al.*, 1998]. The objectives of this experiment, called A Mediterranean Undercurrent Seeding Experiment (AMUSE), were to identify meddy formation sites, estimate the frequency of meddy formation, and investigate processes *other* than meddies that lead to the spreading of MW into the ocean interior. Summarizing what has been learned to date from these data, meddy formation sites were found at two promontories along the Portuguese continental slope, namely Cape St. Vincent and the Estremadura Promontory [*Bower et al.*, 1997a]. Between 15 and 20 meddies were estimated to form per year at these two sites, and meddy formation at Cape St. Vincent appeared to occur when the undercurrent speed was high. Similarity of the relative vorticity in the undercurrent and in the meddies supported the formation mechanism proposed by *D'Asaro* [1988], whereby anticyclonic vorticity is generated by frictional torque along the slope, and anticyclonic eddies are formed when the boundary undercurrent separates at a sharp corner. Newly formed meddies, which at least initially can be detected from satellite altimetry [*Oliveira et al.*, 2000], generally drift away from Cape St. Vincent toward the north or northwest, then turn southwestward and frequently collide with seamounts [*Richardson et al.*, 2000].

[6] In the present study, our main goal is to obtain a better understanding of MW spreading around the Iberian Peninsula due to factors other than meddies. We consider mainly the substantial fraction of the AMUSE float data as well as other float observations from the Iberian Basin that were obtained from *outside* meddies (87%), and investigate the spreading pathways and processes of MW *not* trapped in meddies. A number of recently published studies attempt to infer the main spreading pathways of MW in the Iberian Basin based mainly on hydrographic data [*Zenk and Armi*, 1990; *Daniault et al.*, 1994; *Shapiro and Meschanov*, 1996; *Mazé et al.*, 1997; *Iorga and Lozier*, 1999a, 1999b]. The float data have a certain advantage in that they provide direct observations of absolute velocity and fluid particle pathways. In section 2, the float data set is briefly reviewed, along with two other data sets that are used to augment the AMUSE float data. In section 3, we first describe the cross-stream structure and downstream evolution of the Mediterranean Undercurrent based on hydrographic and float observations. We then illustrate the dominant pathways of MW spreading away from the boundary, as well as the average rate and direction of MW dispersion. Then, we describe a relatively common mechanism revealed by the float trajectories whereby meddies *indirectly* cause MW *not* in meddies to leave the slope and enter the ocean interior. Finally, pseudo-Eulerian and Lagrangian statistics for the circulation at the MW level are presented. In section 4, the float-based results are compared to the hydrography-based views of MW circulation around the southwestern Iberian Peninsula. A summary is given in section 5.

2. Data and Methods

[7] The primary data analyzed in this study consist of RAFOS float trajectories collected during AMUSE. The float data are described in detail by *Bower et al.* [1997a] and *Hunt et al.* [1998]. In brief, this data set includes 44 trajectories of floats deployed in the Mediterranean Undercurrent south of Portugal and tracked acoustically for up to 11 months. The floats were launched in pairs and triplets on a quasi-weekly schedule between May 1993 and March 1994. All the floats were launched within 10 km of 36.5°N, 8.5°W (see Figure 1). The focus of AMUSE was on the lower of the three salinity cores of the undercurrent (see section 3 for definitions), and thus we restrict our attention to data between 950 and 1250 dbar. For some of the analyses that follow, all the data in this pressure range were utilized, but since the main focus here is on processes not directly related to meddies, the tracks were also conditionally sampled in an attempt to eliminate observations directly in meddies. This was done visually by removing track segments with two or more consecutive anticyclonic loops with periods typical of meddies (about 3–20 days).

[8] For the statistical analyses, the AMUSE float data were augmented with RAFOS float tracks from the Medi-

terranean Water level in the Iberian Basin, collected by W. Zenk at the Institut fur Meereskunde Kiel between 1992 and 1994 (see the review by *Käse and Zenk* [1996]). Both float data sets consist of high-resolution trajectories with 1–3 position fixes per day, as well as temperature and pressure measurements.

[9] Finally, we also make use of a hydrographic survey conducted in May 1993 from the *R/V Oceanus* in the western Gulf of Cadiz, also part of AMUSE (see Figure 1 for survey location; also data report by *Bower et al.* [1997b]). This survey consisted of 113 conductivity–temperature–depth (CTD) casts to the bottom or 2000 dbar, and included a number of high-resolution transects across the continental slope and the path of the outflow. The main purpose of this survey was to find an appropriate launch site in the undercurrent for RAFOS floats. However, the data also provide useful information on the downstream evolution of the Mediterranean outflow where it is evolving from a bottom-intensified density current to an intermediate-depth boundary undercurrent.

3. Results

3.1. Transition of the Mediterranean Outflow From a Density Current to an Intermediate-Depth Jet

[10] Previous work has indicated that the Mediterranean outflow approaches neutral buoyancy along the southern Portuguese continental slope [*Ambar and Howe*, 1979a; *Baringer and Price*, 1997], specifically in the vicinity of Portimão Canyon, near 8.5°W. It has also been suggested that Portimão Canyon may act to initiate flow instabilities that eventually grow and form meddies [see, e.g., *Cherubin et al.*, 2000; *Serra and Ambar*, 2002]. Here we investigate the synoptic structure of the outflow in this critical and complex area using the AMUSE hydrographic data described above. These field data provide exceptionally high cross-slope resolution with station spacing about 3 km across the undercurrent. The bottom slope in the 200–2000 m depth range increases dramatically through this region, by a factor of four between 7°W and Portimão Canyon at 8.5°W (Figure 1). As will be seen below, this leads to a narrowing of the Mediterranean Undercurrent, necessitating close station spacing to resolve its hydrographic and flow structure.

[11] The pathway of MW through the western Gulf of Cadiz during May 1993 can be seen in Figure 2, which shows the properties at the pressure of the absolute salinity maximum below 500 dbar. Stations where the salinity maximum has lifted off the bottom are indicated by white dots. Some stations have multiple salinity maxima associated with different cores of MW. Previous studies have identified three cores or veins: a small shallow core, and the main upper and lower cores, at approximate depths 400 m, 700 m and 1200 m and densities $\sigma_0 = 27.40$, $\sigma_1 = 31.85$ and $\sigma_1 = 32.25$, respectively (after reaching neutral buoyancy) [see, e.g., *Ambar*, 1983; *Ambar and Howe*, 1979a, 1979b]. Since our survey was mostly in water at or deeper than 1000 m, our focus here is on the lower core, which transports about 60% of the salt flux [*Daniault et al.*, 1994]. Furthermore, the lower maximum is saltier and cooler than the upper, thus in general, where there are multiple maxima, Figure 2 shows the properties of the lower core.

[12] The pathway of the most saline MW generally followed the slope from southeast to northwest through the middle of the study area, indicated for example by the swath of salinities greater than 36.6 (yellow and red shading in Figure 2a). The low salinity feature at 36°30′N, 7°45′W is coincident with a small topographic high (not visible in isobaths drawn here) [see *Ambar and Howe*, 1979a, Figure 1], which apparently forces the main outflow to its south. East of about 8°10′W, the high-salinity vein was entirely against the seafloor (indicated by black station dots coincident with red and yellow shading, $S_{max} > 36.6$), whereas to the west of that meridian, some parts of the saltiest outflow had started to float off the bottom (indicated by white station dots). S_{max} (Figure 2a) and the density of S_{max} (Figure 2b) decreased rapidly along the outflow path between 7°30′W and 8°10′W, where it was still in contact with the seafloor, from about 37.1 salinity, 32.5 σ_1 at station 7 (along 7°30′W) to 36.7, 32.3 σ_1 at 8°10′W. This transition in properties coincides with a sharp steepening of the topography: the cross-slope separation of the 1000 and 1400 m isobaths decreases from about 40 km at 7°30′W to about 16 km at 8°W. Considering the plume model work of *Price and Baringer* [1994] and others, a local acceleration due to buoyancy forces, and enhanced entrainment is likely here, which would cause a narrowing of the plume, and a local decrease in salinity and density as observed. In fact, the path of the saltiest water appears to be downslope in this region. This entrainment event decreases the density enough to match the ambient stratification, and some parts of the outflow start to separate from the seafloor near 8°10′W. Upon entering Portimao Canyon, the bottom slope increases still further, and the entire lower core lifts off (see more discussion below). Salinity of the outflow remained relatively constant through and west of Portimao Canyon, with S_{max} values 36.6–36.7, suggesting that dilution by turbulent entrainment was negligible along this part of the path.

[13] Near 8°10′W, the densest outflow waters, with $\sigma_1 > 32.3$, apparently split north and south of a bathymetric high point centered at about 36°12′N, 8°20′W (labeled "A" in Figure 2a). Just upstream of the bump is a canyon, at the head of which the 1200 and 1400 m bathymetric contours sharply converge, creating a locally steep slope. Comparing salinity, density and pressure of the salinity maximum in the vicinity of this canyon (Figures 2a–2c), the southern branch was apparently "drained off" from the main body of MW and plunging down this steep slope, rapidly losing its salinity anomaly through enhanced entrainment, and floating off the bottom. A northern branch with similar density continued westward more along the isobaths into the Portimão Canyon complex, also deepening and floating off the bottom, but maintaining more of its high salinity anomaly. It continued around a second, smaller bathymetric ridge (36°25′N, 8°15′W; "B"), partially looped through Portimão Canyon, then continued westward along the slope.

[14] This high-density, high-salinity MW (with $\sigma_1 > 32.3$) is somewhat denser than the traditional lower core water, which has $\sigma_1 = 32.25$ [*Zenk and Armi*, 1990]. Figure 3 shows profiles of σ_1 versus salinity for all stations where S_{max} was floated off the bottom (white dots in Figure 2). A number of profiles cluster together illustrating the denser salinity maximum, with $\sigma_1 > 32.3$, $S_{max} > 36.6$. The salinity

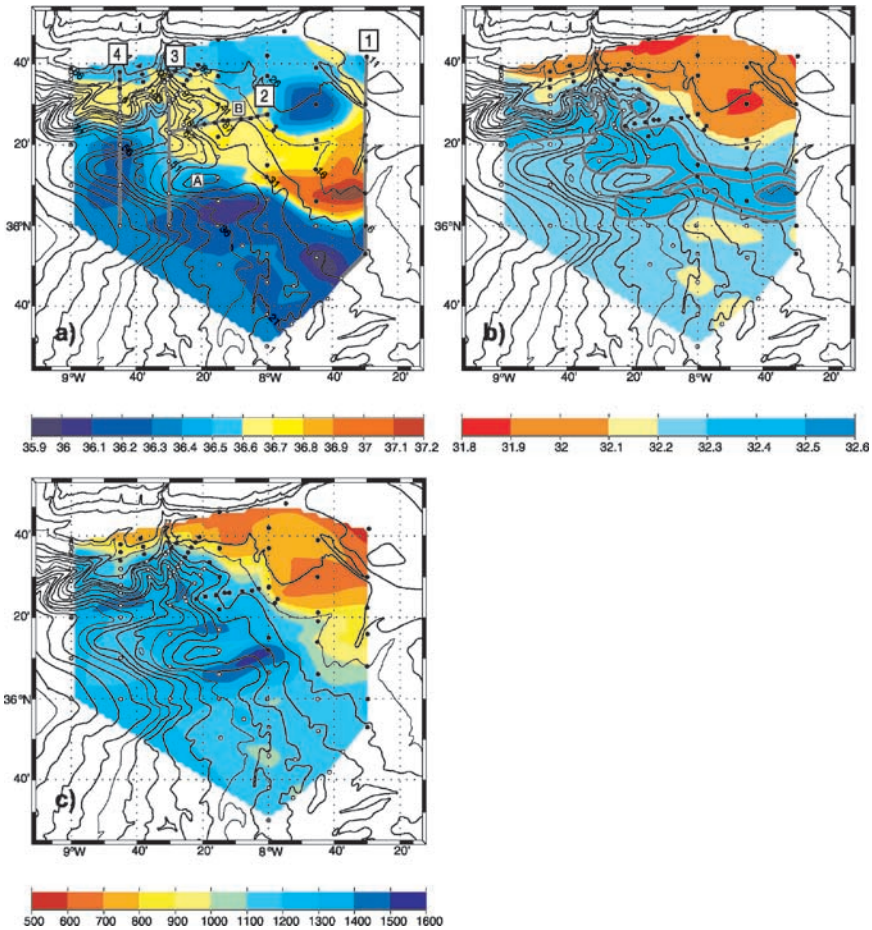

Figure 2. Properties at the level of the salinity maximum below 500 m from AMUSE hydrographic survey during May 1993 in the region shown by the box in Figure 1. Color shading indicates property values, and black contours show bathymetry every 200 m, highlighted every 1000 m. Dots indicate station positions, and are unfilled where the salinity maximum is more than 100 m above the seafloor. Locations of four high-resolution cross-sections shown in Figures 4 and 5 are highlighted, as well as the locations of two topographic bumps, "A" and "B". (a) salinity, (b) potential density (σ_1), where three density levels are highlighted with gray contours, (c) pressure (dbar).

maximum with the traditional density of 32.2–32.3, lying above and onshore of this denser vein, floated off the bottom farther downstream, starting at about 8°15′W, i.e., in the eastern part of the Portimão Canyon complex, where the slope steepens again (1000–1400 m isobath separation here is only about 5 km).

[15] Vertical sections of salinity and density across the outflow further illustrate the transition of the Mediterranean outflow from a bottom-trapped density current to an intermediate-depth jet, Figure 4 (see Figure 2a for section locations). At section 1 (Figure 4a), the dense, high-salinity outflow plume (yellow and red shades) was entirely against the seafloor over a distance of about 80 km, including stations 11-6. Outflow waters denser than $\sigma_1 > 32.2$ were observed in a 100 m-thick layer at station 7 (water depth 1000 m), and in a much thinner layer at station 9 (800 m). Cross-stream variations in the outflow properties arise due to differences in the properties of the overlying water where the outflow is spread out along the slope [*Baringer and Price*, 1997]. At section 2, just upstream of Portimao Canyon (Figure 4b), the isolated density contours had disappeared, and the outflow pathway was split around the small spur near 36°25′N, 8°15′W ("B"). Here the denser vein of MW ($\sigma_1 > 32.3$, S > 36.6, θ = 11.7C) was forced to flow around the western end of the spur (stations 82 and 50; see also Figure 2a), while less dense MW, more typical of the lower core (σ_1 = 32.2–32.3, S > 36.6 and θ = 12.2 C) was found over the small ridge and through a small gap at the eastern end of the ridge (bracketed by stations 85 and 88). Note that the denser salinity maximum (stations 82 and 50) had descended about 300 m from the 1000-m depth of the salinity maximum in section 1, to a depth of 1300 m. The denser MW had floated off the seafloor, as evidenced by the suspended salinity maxima, while the traditional lower core of MW was still against the bottom.

[16] The traditional lower core salinity maximum floated off the bottom as it entered Portimão Canyon, as shown for section 3 at 8.5W, stations 46 and 47 (Figure 4c). The complex topography found at section 2 is replaced here with a single, very steep slope, causing the cores at different depths to be nearly aligned vertically. The density structure indicates a subsurface geostrophic jet flowing perpendicular to the section by the downward slope of the 32.2–32.3 σ_1 contours and the upward flaring of the 31.9– 32.1 contours

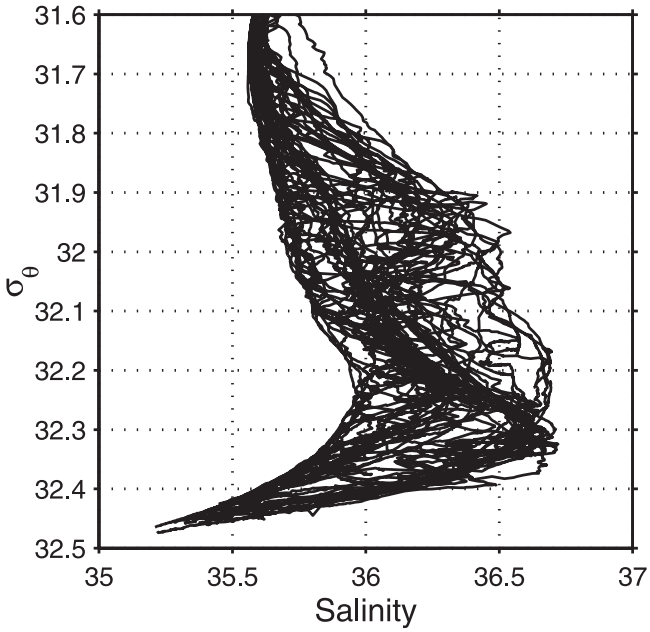

Figure 3. The σ_1–S profiles for all stations where the salinity maximum was lifted off the seafloor, locations indicated by white dots in Figure 2a. A group of stations has a salinity maximum with $\sigma_1 > 32.3$, denser than the traditional MW lower core.

within 20 km of the continental slope. This implies a westward velocity maximum at about 1100 dbar. A similar density structure at section 4, 8.75° W (Figure 4d) indicates the continuation of the undercurrent along the slope, centered at about 1000–1200 dbar. Note that between sections 2 and 4, the depth range of maximum salinities (S > 36.6), 1000–1400 dbar, does not change much, whereas at section 1, the saltiest water was all shallower than about 1200 dbar.

[17] Figure 5 shows geostrophic velocity (black contour lines) perpendicular to the same four cross-sections, superimposed on salinity (color shading). Traditionally, investigators have used the salinity minimum above the outflow as a level of no motion across the section when referencing geostrophic calculations [*Heezen and Johnson*, 1969; *Ambar and Howe*, 1979a, 1979b]. More recently, *Baringer and Price* [1997] used the constraint of zero net salt flux across sections farther upstream (closer to Gibraltar) to find a level of no motion. They found that the reference level determined in this way was quite close to the salinity minimum (within 100 m). In light of their results, we have used the salinity minimum as a level of no motion across the sections.

[18] Section 1 (Figure 5a) indicates westward velocities in a 200-m thick, 80-km wide layer above the bottom that corresponds to the high-salinity water, with maximum westward speeds exceeding 0.2 m s^{-1}. Moving downstream to section 2 (Figure 5b), which is oriented more perpendicular to the isobaths, the highest downstream velocities, exceeding 0.4 m s^{-1}, were associated with the lower core salinity maximum at stations 88–91. Narrow bands of alternating upstream and downstreamflow predominated over the small ridge (including a bottom–intensified vein near the small depression at station 87), and the denser MW at the nose of the ridge was flowing downstream more slowly than the traditional lower core vein farther inshore. The horizontal scale of the downstreamflow appears to have decreased substantially relative to the upstream section, from about 80 km to about 15 km for the individual veins at section 2, due to the increase in the bottom slope. At section 3 (Figure 5c), the bottom slope has increased more, and the along-slope flow appears as a very narrow, ~10 km-wide band with maximum downstream speed of just over 0.4 m s^{-1} centered at about 1100 m depth. There is evidence of downstreamflow associated with the upper core at depths 700–1000 m at the very inshore edge of the section, although this is not well-resolved. The downstreamflow greater than 0.1 m s^{-1} between stations 50 and 51 is probably associated with the flow around the nose of the small spur discussed above, as this section cuts across its western end (see Figure 2a). Finally, section 4 (Figure 5d) reveals the continuation of a strong, narrow, westward jet close to the slope centered at about 10 km along the section. Just offshore was a narrow band of opposing flows less than 10 km wide, with maximum velocities centered at 1200–1400 m depth. This could be a small meddy, as the velocity signature is associated with a lens-like density distribution with a high salinity core that has separated from the slope (see Figure 4d, station 57 at ~22 km, 1100–1300 dbar). This is in the density range of the densest MW, σ_1 = 32.25–32.35. The strong deep eastward flow centered at 30 km along this section may be associated with a deep countercurrent as described also by *Ambar and Howe* [1979b] and *Ambar et al.* [2002]. These synoptic observations of the undercurrent structure will be compared to the mean structure derived from float data in the section 3.2, and discussed further in section 4.

3.2. Direct Velocity Observations in the Mediterranean Undercurrent

[19] The AMUSE RAFOS floats provide independent, direct measurements of the velocity structure of the Mediterranean Undercurrent and variability that can be compared with the geostrophic calculations described above. Figure 6 shows all the nonmeddy, lower-core (as defined in section 2) float velocity observations around the southwestern Iberian Peninsula. Note that float speed was calculated as a centered difference between position fixes 16 hours apart, and therefore represents an average over that time period. Speeds in excess of 0.3 m s^{-1} (red dots) were frequently observed in the undercurrent south of Portugal (Region 1). However, over the western Portuguese slope between St. Vincent's Canyon (37°N) and Lisbon and Setubal Canyons (38.2°N) (Region 2), float speed only occasionally exceeded 0.2 m s^{-1} near the boundary. Northwest of these canyons, along the southern flank of the Estremadura Promontory, higher speeds were again observed, with values frequently greater than 0.2 m s^{-1} and occasionally greater than 0.3 m s^{-1}. These differences most likely result from changes in bottom slope, which is steep south of Portugal and southwest of the Estremadura Promontory, and less steep between Cape St. Vincent and the promontory (see Figure 1). The formation of meddies at Cape St. Vincent may also contribute to the overall decrease in undercurrent speed between the southern and western Portuguese continental slopes.

[20] The cross-slope (cross-stream) structure of the undercurrent is illustrated in Figure 7 for the two regions indicated by boxes in Figure 6, one upstream and the other

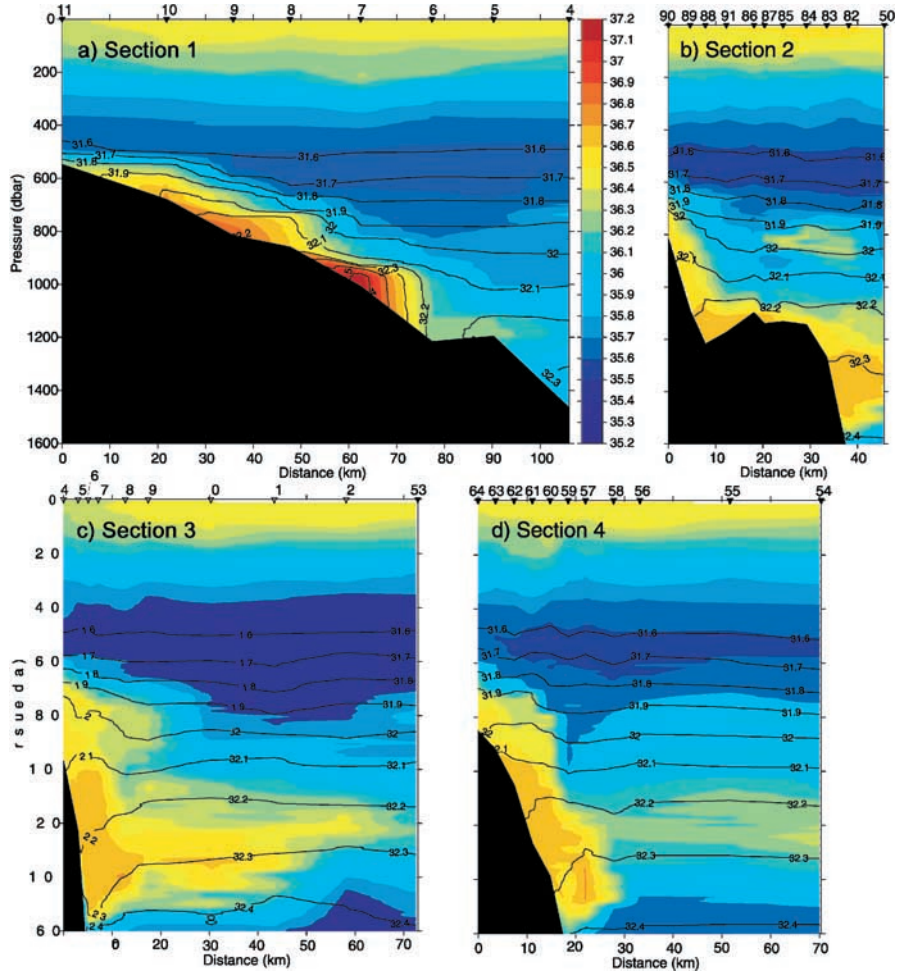

Figure 4. Vertical distributions of salinity (color shading) and density ($\sigma_1 \geq 31.6$, black contours) along four sections south of Portugal (see Figure 2a for section locations). Same color scale applies to all sections. (a) section 1, (b) section 2, (c) section 3, (d) section 4. Station locations and numbers are indicated along top axis. These sections illustrate the transition of the MW outflow from a bottom-trapped density current in section 1 to an intermediate-depth salinity maximum in sections 2–4.

downstream of Cape St. Vincent. Figure 7a shows zonal velocity as a function of meridional distance from 36.8°N, along with the mean cross-stream profile and standard deviation in 10-km bins. The most striking feature is the large variability. Between 20 and 40 km, maximum zonal float speed exceeded -0.4 m s^{-1} in the downstream (westward) direction (negative values), and 0.1 m s^{-1} in the upstream (eastward) direction (positive values). In the mean, a jet-like structure emerges in spite of the strong variability, with peak speed of about -0.2 m s^{-1}, decreasing to zero in the offshore direction over a distance of about 30 km. Although mean velocity also decreases to zero inshore of the jet maximum, this feature of the mean structure is not robust due to the small number of observations. Standard deviation in the jet is large, about 0.1 m s^{-1}. The corresponding temperature observations, Figure 7b, show the highest float temperatures, exceeding 12.5°C, mostly associated with the jet maximum. Again note the large variability, even at the jet maximum, where temperatures as low as 10.5°C were observed, reflecting the lateral entrainment of cooler offshore water into the undercurrent (see section 3.4 below).

[21] The maximum float speeds in the undercurrent south of Portugal were similar to the peak geostrophic velocity observed in hydrographic section 4, 0.4 m s^{-1}. Recent direct velocity observations made with a Lowered Acoustic Doppler Current Profiler (LADCP) in and around Portimão Canyon described by *Cherubin et al.* [2000] reveal generally faster current speeds at the head of the canyon (not well-sampled by the floats) compared to farther downstream. The width of the mean jet determined from the float data (from jet maximum to zero crossing, ~30 km) is wider than the ~10-km width observed in the synoptic geostrophic sections west of 8.5W. However, note that about 80% of the float observations with zonal speed >0.2 m s^{-1} westward were located in a very narrow, 15-km wide band (see also cluster of red dots south of Portugal in Figure 6). Inspection of individual float tracks reveals that some relatively fast-moving floats were diverted away from the slope due to a meddy forming downstream, which may account for the wider mean jet in Figure 7a.

[22] The velocity structure of the undercurrent along the western Portuguese slope differs dramatically from that upstream of the cape (Figure 7c). As shown qualitatively

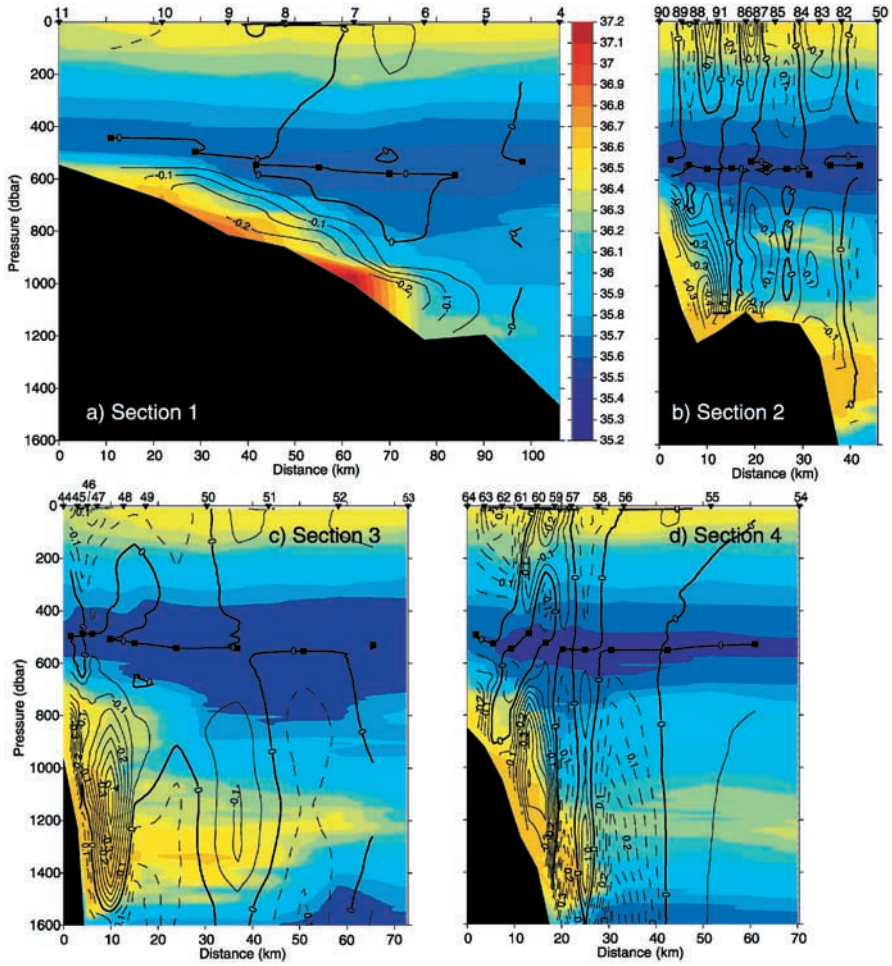

Figure 5. Same as Figure 4 but showing salinity (color shading) and geostrophic velocity (black contours). Contour interval for velocity 0.05 m s^{-1}. Negative values (solid contours) are downstream (generally westward). Solid squares show the salinity minimum, used as the level of no motion across the section. The velocity structure of the outflow narrows dramatically to about 10 km wide in Portimao Canyon, section 3.

in Figure 6, almost all float speeds were less than 0.2 m s^{-1} northward between St. Vincent's Canyon and Lisbon/Setubal Canyons. *Southward* velocities exceeding 0.1 m s^{-1} were also observed, and the mean velocity has a maximum value that is just 1/3 of that along the southern slope, about 0.06 m s^{-1}. Furthermore, the jet-like structure is absent, replaced by an at least 50-km wide band of northward flow between 0.04 and 0.06 m s^{-1}. Maximum temperatures here were also lower, all <12.5°C (Figure 7d), reflecting the dilution of MW due to mixing as the undercurrent flows around Cape St. Vincent. While others have noted the general decrease in undercurrent speed around Cape St. Vincent [see, e.g., *Cherubin et al.*, 2000], the large number of float observations from AMUSE reveal not only the reduction in peak mean velocity, but the change in velocity structure as well.

3.3. Mediterranean Water Spreading Pathways and Rates

[23] We now shift attention to the larger-scale spreading of MW as revealed by the AMUSE float tracks. Figure 8 shows the dispersal of lower-core floats from their launch position in the Gulf of Cadiz (launch site indicated by "x") as a function of elapsed time after launch. Also in this figure, floats that ended up in meddies as well as those that did not are included, to give a view of the dispersion of MW due to all processes.

[24] The tight cluster of tracks extending westward from the launch site indicates that most of the floats were initially advected directly westward parallel to the slope toward Cape St. Vincent (Figures 8a and 8b). Some did not make it to the cape however: almost one-third of the floats (9/30) drifted offshore into the Gulf of Cadiz before rounding Cape St. Vincent, indicative of some "leakage" of MW from the undercurrent into the gulf.

[25] More wide-spread dispersal is evident as the floats passed St. Vincent Spur at 9.5°W (Figure 8b). Of the floats that passed through the "gateway" between St. Vincent's Spur and Gorringe Bank [*Zenk and Armi*, 1990], some turned sharply northward and continued along the continental slope, and others shot offshore toward the west–northwest. After 60 days, three spreading pathways are evident; southward from the launch site, west–northwestward from St. Vincent's Spur, and northward along the western Portuguese slope (Figure 8c). After four months,

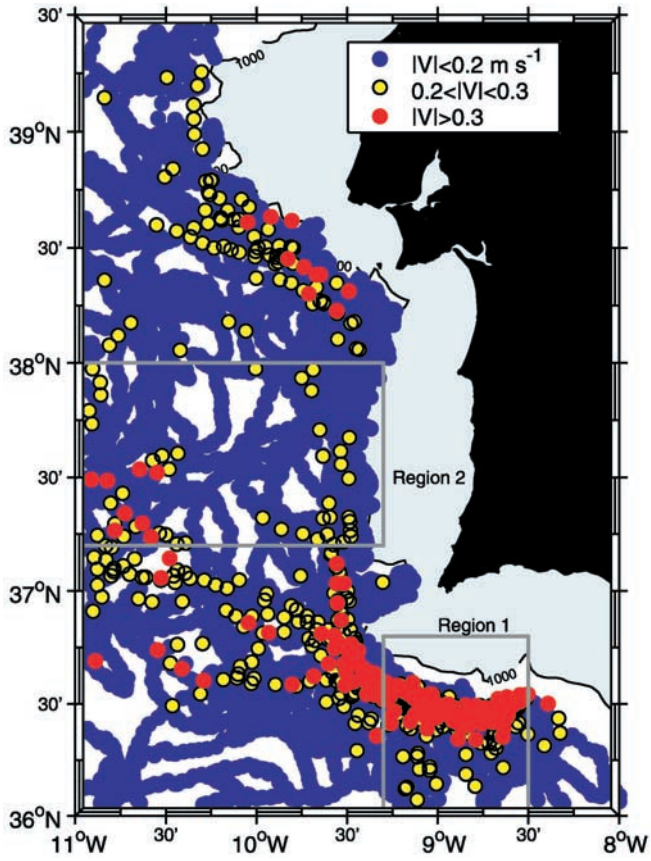

Figure 6. Spatial distribution of velocity at the lower core level (950–1250 dbar) from nonmeddy AMUSE RAFOS float observations. Dots indicate locations of velocity observations, and color indicates magnitude in three ranges: red $|\mathbf{V}| > 0.3$ m s^{-1}; yellow $0.2 < |\mathbf{V}| < 0.3$ m s^{-1} and green $|\mathbf{V}| < 0.2$ m s^{-1}. Boxes indicate two regions where the cross-stream structure of the undercurrent is determined from the float data (Figure 7). The 1000 m isobath is also shown. Peak speeds in the undercurrent decrease significantly from upstream to downstream of Cape St. Vincent, in part due to a decrease in bottom slope.

Figure 8d, about 30% of the floats were still south of the latitude of the launch site, in and west of the Gulf of Cadiz (8/25), about 60% were spread over the Tagus Abyssal Plain from the boundary to about 14°W, and only about 10% were north of the Estremadura Promontory. After eight months, Figure 8f, the number of available floats dropped to 13, but the general distribution remained the same: about 30% were south of the launch site, and the rest west of the Iberian Peninsula.

[26] A remarkable feature of Figure 8 is the large fraction of floats that left the continental slope within four months: all but 3 floats, or 22/25, were offshore of the 4000-m isobath. This illustrates the significant amount of mixing of lower-core MW that occurs in this region. Part of this is due to the formation of meddies near the boundary and their translation into the interior. But many floats left the boundaries that were not trapped in meddies. Figure 9 shows some of the persistent pathways followed by floats not trapped in meddies. Four floats that left the undercurrent before passing through the gateway are illustrated in Figure 9a. Three of these floats were initially advected westward in the undercurrent, but then turned southward into the Gulf of Cadiz. The fourth float drifted due south from the launch site, suggesting a major disruption of the canonical undercurrent structure. Analysis of other floats launched at that time and the contemporaneous expendable bathythermograph (XBT) observations indicate such a disruption [*Ambar et al.*, 1999].

[27] A significant number of floats left the boundary toward the west–northwest at the spur: four examples are shown in Figure 9b. In some cases, these floats continued to measure the warm temperatures associated with the undercurrent as they crossed the "gateway" and passed north of Gorringe Bank, suggesting that relatively undiluted MW *not* in meddies is being directly injected into the ocean interior from this location. Some floats that rounded the spur drifted northward along the boundary in what appears to be a continuous undercurrent between the launch site and 38°N, where Lisbon and Setubal Canyons indent the slope and the large-scale orientation of the slope changes from north–south to northwest–southeast (Figure 9c; also shown by *Richardson et al.* [2000]). From this location, all four floats crossed the slope into deeper water, and none continued along the slope around the promontory.

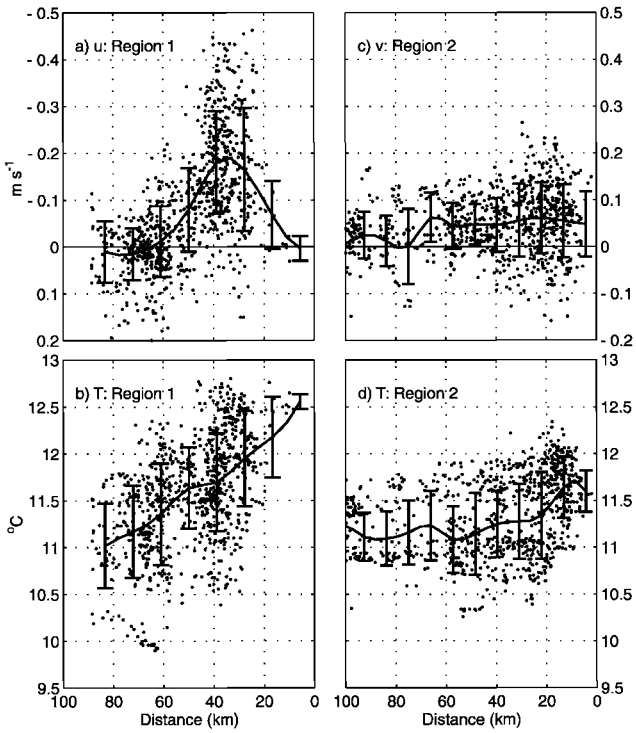

Figure 7. Cross-stream structure of the Mediterranean Undercurrent based on nonmeddy AMUSE RAFOS float observations. (a, b) Zonal velocity (positive eastward) and temperature as a function of meridional distance from 36.8°N (positive offshore) for Region 1, located south of Portugal (see Figure 6). Error bars indicate standard deviations in 10-km cross-stream bins. (c, d) Same as (a, b) but for Region 2, and showing meridional velocity (positive northward) as a function of zonal distance (positive offshore).

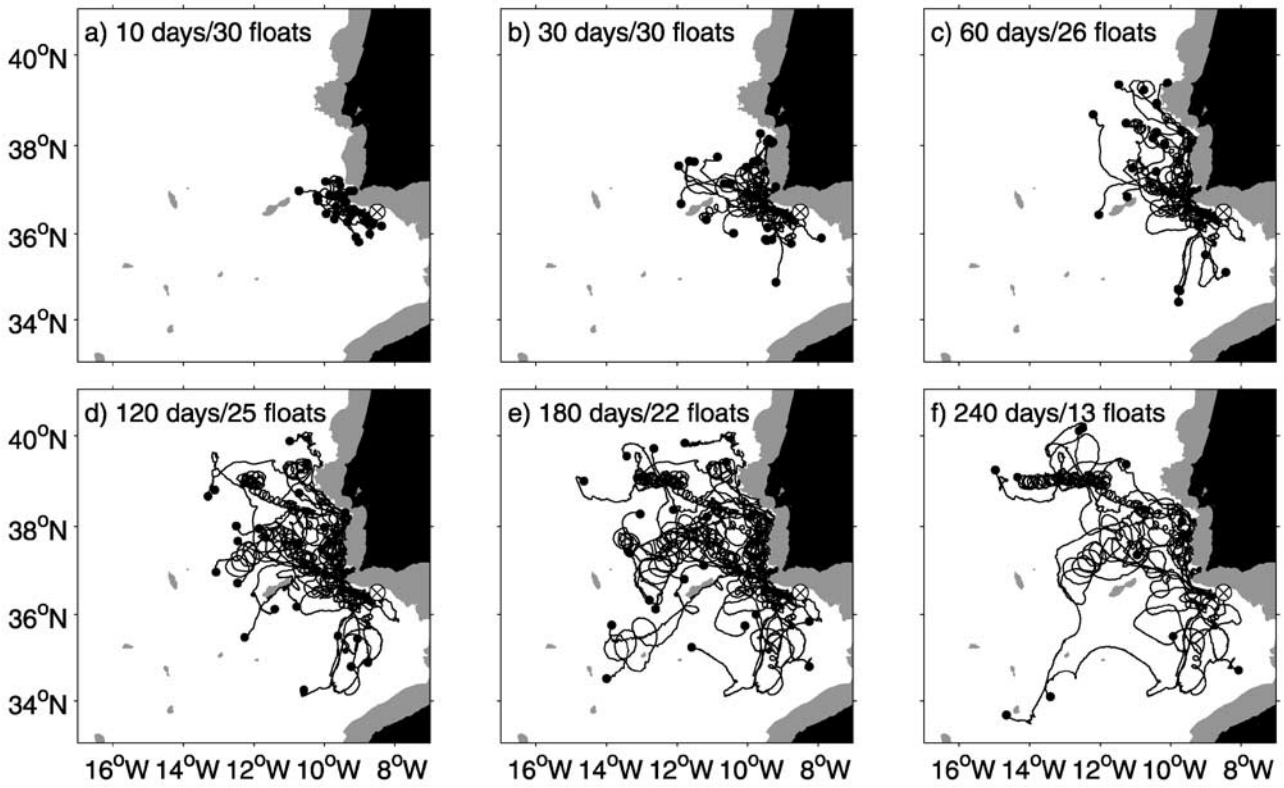

Figure 8. Trajectories of all meddy and nonmeddy floats at the lower core level from AMUSE as a function of elapsed time since launch at the "x". Solid dots indicate end positions. Gray shading indicates the 1000 m isobath.

[28] The float trajectories are valuable because they not only show directly the fluid parcel pathways, but also often reveal the process by which water masses are stirred and mixed. For example, there is evidence in the AMUSE trajectories that the presence of forming or recently formed meddies (and in some cases a companion cyclone) [see *Serra et al.*, 2002] against the boundary has a major impact on the dispersal of MW not in meddies. This was shown by *Bower et al.* [1997a] for a meddy situated against the slope northwest of the Estremadura Promontory. Here we show three examples of how this also occurs at Cape St. Vincent (Figures 10–12). Basically, in all three cases, the presence of a meddy over the slope caused MW approaching the meddy from upstream in the undercurrent to be deflected offshore along the southern rim of the meddy. Each figure shows a series of "snapshots" of all float tracks in the vicinity of Cape St. Vincent during these blocking events.

[29] Figure 10a shows a group of floats drifting relatively smoothly westward from the launch site to St. Vincent Spur, and then rounding the spur toward the northwest. Ten days later, Figure 10b, float 138 completed a small anticyclonic

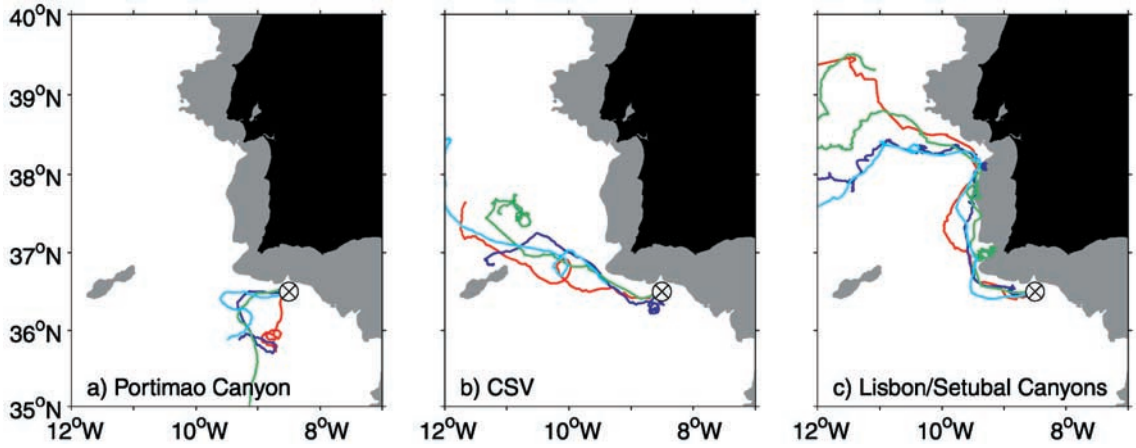

Figure 9. Examples of persistent pathways of AMUSE floats, showing where floats are most likely to leave the boundary. Gray shading indicates 1000 m isobath.

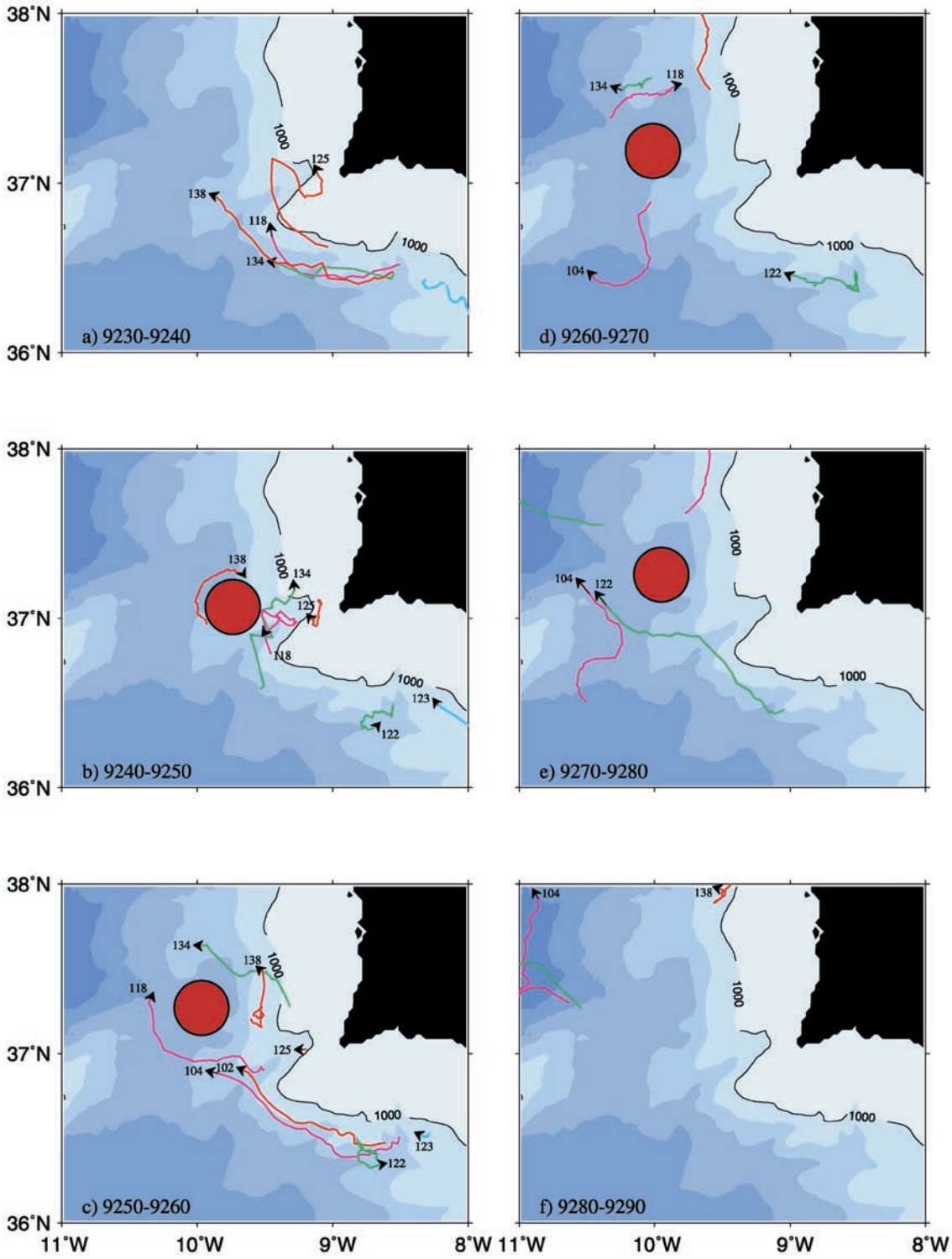

Figure 10. Series of "movie frames" showing the evolution of the flow field around the southwestern Iberian Peninsula in 10-day increments. All AMUSE floats that were available are used. Numbers near arrowheads indicate float number, and the dates are in modified julian day (lower left corner). Red circle shows position of possible meddy. Bathymetry shaded in 1000 m intervals.

half-loop, while float 118, 125 and 134 stalled in St. Vincent's Canyon. A red circle has been drawn to indicate the location of a possible meddy or meander inshore of float 138. In the next 10 days (Figure 10c), float 118 starts a larger anticyclonic half-loop, which it completed during the following 10 days (Figure 10d), also suggesting the presence of a meddy. In Figures 10c and 10d, floats 102 and 104, approach the spur from upstream and are deflected offshore, possibly as a result of this feature (float 102 ended its mission during this time). The meddy was apparently still blocking the

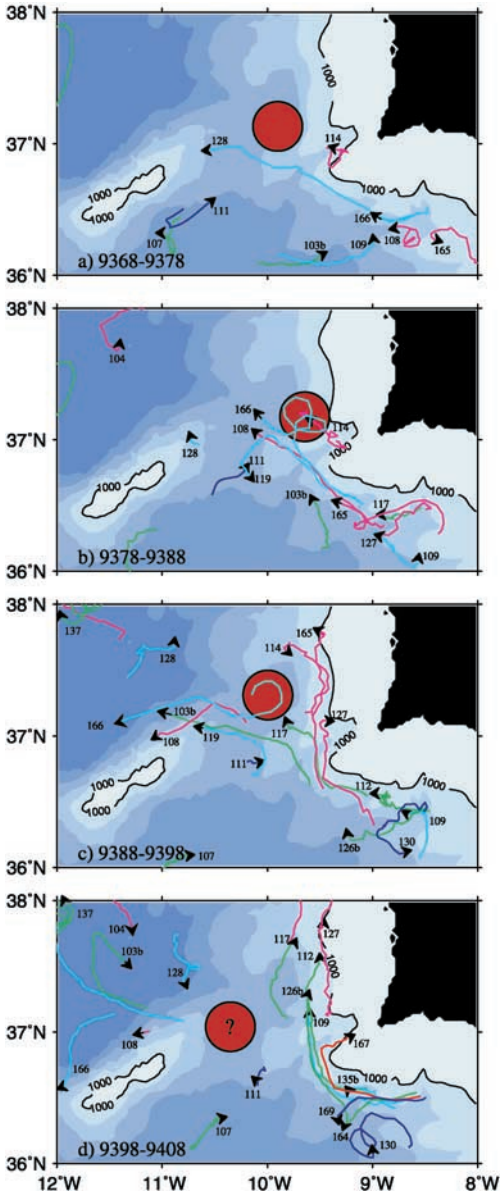

Figure 11. Same as Figure 10 but for a different set of floats. In this case, one float (#166) was temporarily trapped in the meddy, confirming its position.

undercurrent for at least 10 more days (Figure 10e), as float 122 (with 104) was also diverted offshore as it approached from upstream. Both floats 104 and 122 were "permanently" lost from the undercurrent, as they continued to drift westward and northwestward into the interior (Figure 10f).

[30] In the above example, none of the floats were actually trapped in this possible meddy, which would have helped to confirm its existence. In the next two examples, floats were caught in forming meddies and reveal their exact locations. In Figure 11a, float 128 drifts rapidly offshore from St. Vincent's Spur, and the cusps in its track are suggestive of a possible anticyclonic eddy to the north. This is confirmed in Figure 11b, when float 166 makes two complete anticyclonic loops. Floats 108 and 119 are advected off the slope along the southern rim of the meddy. The cycloidal motion of float 166, that continues in Figure 11c, indicates that the meddy is moving away from the slope. This apparently then allowed the undercurrent to again flow uninterrupted around the spur and northward, illustrated by a number of floats that approached from the Gulf of Cadiz, rounded the spur and drifted northward along the slope (Figures 11c and 11d).

[31] Finally, Figure 12a shows a group of floats again approaching St. Vincent's Spur from the launch site. Floats 129, 135b and 139 all make a relatively large offshore swing as they are advected downstream in the undercurrent. Float 129 is caught in a meddy (Figure 13b). The three floats that approach from upstream, 106b, 120b and 121b, as well as 115 which had previously stalled right against the spur (Figure 12b), were all swept offshore when they encountered the meddy near the spur (Figures 12b and 12c). These were

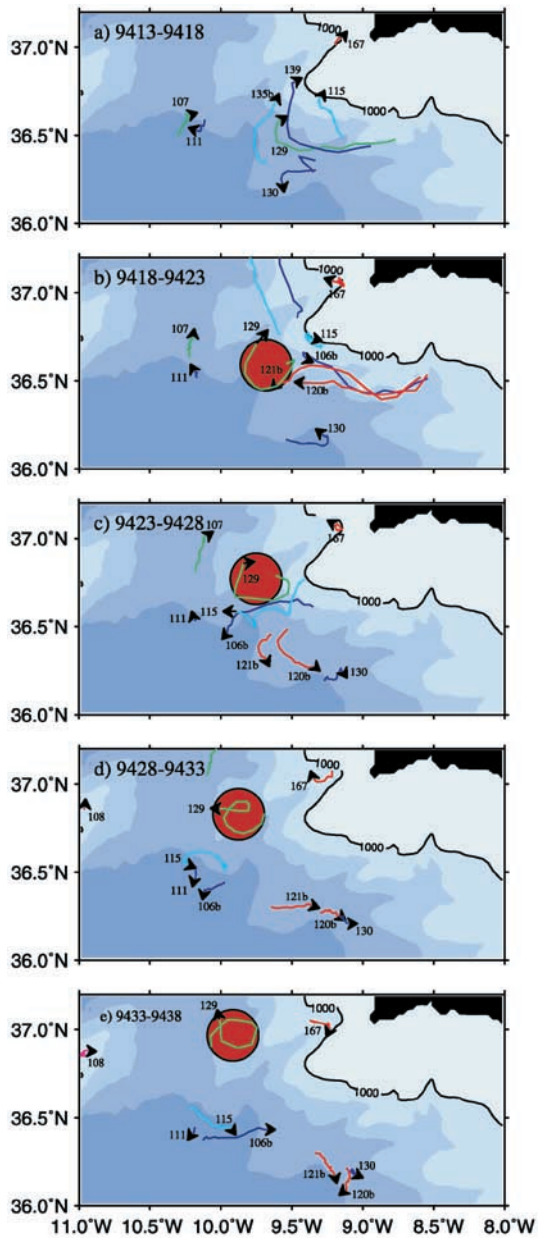

Figure 12. Same as Figure 11, but showing flow around a different meddy near Cape St. Vincent. Float #129 was caught in the meddy.

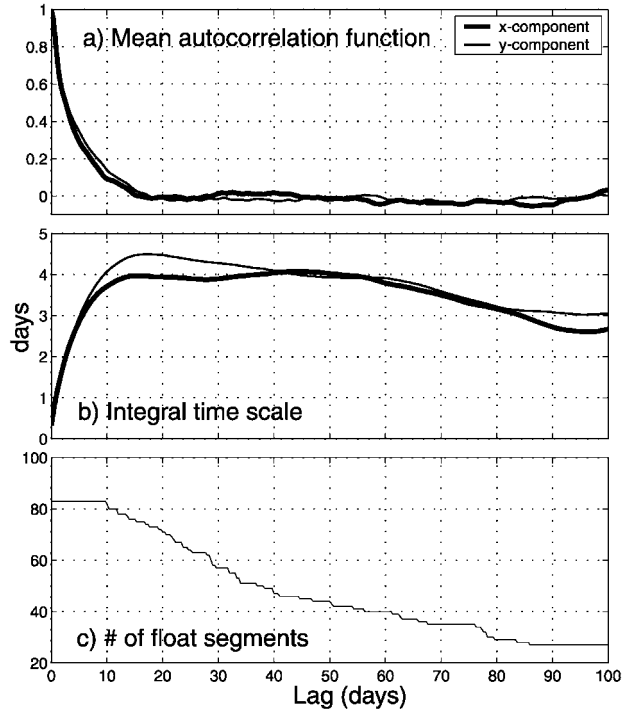

Figure 13. (a) Mean zonal (thick line) and meridional (thin line) velocity autocorrelation functions as a function of time lag from all nonmeddy floats at the lower core level. (b) integral of (a); (c) number of float track segments.

the last floats to be launched in the undercurrent in this experiment, so the resumption of "normal" boundary undercurrent flow around the spur and northward seen in the previous case was not observed. Based on these observations of "meddy blocking," we conclude that two of the three prominent MW pathways illustrated in Figure 9, those directed southward into the Gulf of Cadiz and westward from St. Vincent Spur, are most likely caused by the formation of meddies near the spur.

[32] The average spreading rate of MW in the lower core has been estimated by calculating the velocity of the center of mass of the floats illustrated in Figure 8 as a function of time since launch. Note that these estimates do not represent mean velocities for this region, rather they indicate the average rate at which MW spreads away from the float launch site via meddies and other processes. The initial spreading of the MW in the lower core of the undercurrent is mainly westward at about 0.15 m s^{-1}. This decreases rapidly and reaches a more or less constant value of 0.01–0.02 m s^{-1} after about 100 days. The meridional spreading is initially northward at about 0.02 m s^{-1}, reflecting the influence of the boundary undercurrent. But the average meridional spreading rate decreases to less than 0.01 m s^{-1} after 100 days. The spreading rate based on the seven floats that were in the water for the longest period (330 days, is 0.016 m s^{-1} at 299T (WNW). When the spreading of MW due to the translation of meddies is considered separately, *Richardson et al.* [2000] estimated a mean speed of 0.02 m s^{-1} toward 227T (SW; this includes both Iberian and Canary Basin meddies). Consideration of nonmeddy processes in MW spreading thus does not change the spreading rate inferred from meddies but the direction is more northward.

3.4. Pseudo-Eulerian and Lagrangian Statistics

[33] The above results have focused on the MW spreading pathways and rates from the Gulf of Cadiz toward the interior. We now shift attention to the larger area sampled by all RAFOS floats (launched as part of AMUSE and by IfM Kiel) around the southwestern Iberian Peninsula. The combined float data set has been used to map the Eulerian mean temperature, velocity and eddy kinetic energy fields at the MW level by averaging the float observations in regularly spaced averaging areas. In an attempt to resolve the details of the circulation, we averaged the data in roughly 0.5° × 0.5° areas (compared to the 1° × 1° averaging areas used by *Sparrow et al.* [2002] in their larger-scale analysis of mean flow at the MW level). Recognizing that close to the boundary, the flow is topographically steered, we grouped the data not only according to horizontal distance from the grid points, but also according to bottom depth, as described by *Davis* [1998]. The effective (nondimensional) "distance" between each float observation (a) and the grid points (b) was calculated according to

$$r^2 = \left|\frac{\mathbf{x}_a - \mathbf{x}_b}{L}\right|^2 + \left[3\mu\frac{H_a - H_b}{H_a + H_b}\right]^2,$$

where x_a and x_b are the coordinates of the data and grid points, H is the water depth, and L and μ are adjustable parameters that determine the relative weight of horizontal separation and water depth differences. Values of L = 110 km and μ = 60 generated a relatively smooth velocity pattern near the boundary. Each observation was then assigned to the "nearest" grid point based on its r value. This technique reduces the variability that would result from averaging together observations of the more rapid undercurrent over the middle continental slope with the generally slower flow over the abyss. Our goal in this analysis was to obtain estimates for the "background" circulation, that is, other than that due directly to meddies, so only the nonmeddy data were used.

[34] Since it is important to know the statistical uncertainties when interpreting the mean fields, some knowledge of the Lagrangian integral timescales for this region is needed. To estimate it, we considered all the float data east of 14°W (the more data-rich region), which include 84 continuous float track segments, ranging in length from 10 to 331 days. The zonal and meridional velocity autocorrelation functions were estimated for each track segment after removing the spatially dependent mean velocity, as also done by *Owens* [1991] and *Spall et al.* [1993]. If the segment means, rather than the spatially dependent mean, were removed, the integral did not converge. The functions were then averaged (weighted by segment length) to obtain the mean autocorrelation and its integral shown in Figure 13 as a function of time lag. The first zero crossings of the zonal and meridional autocorrelation functions occur at time lags of 15–20 days. The integrals of the autocorrelation functions converge well in the range 15–60 days, and indicate an integral timescale of about four days. The autocorrelation functions at long lags are probably dominated by noise.

[35] These estimates for the integral timescales, ~4 days, are remarkably small. In the western North Atlantic, *Owens*

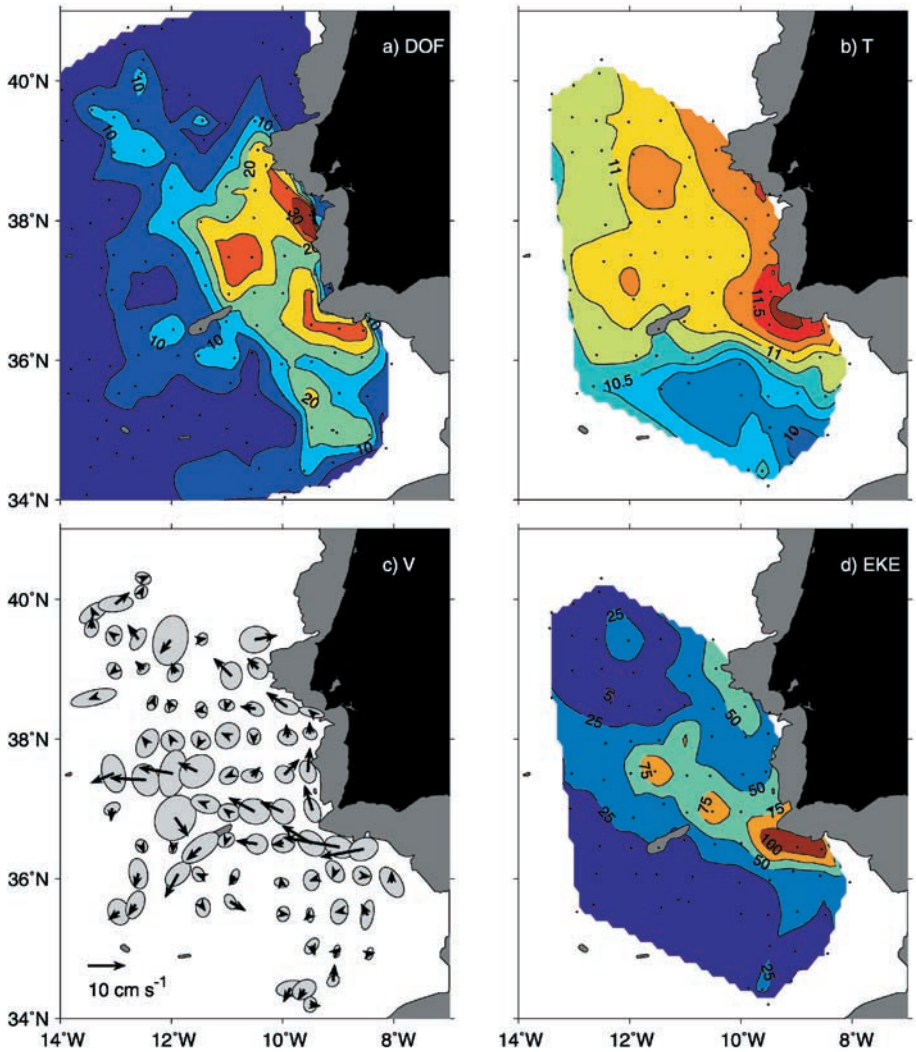

Figure 14. Pseudo-Eulerian statistics based on all nonmeddy AMUSE and IfM float data at the lower core level. (a) Degrees of freedom; (b) mean temperature (°C); (c) mean velocity vectors and 90% confidence ellipses (cm s^{-1}); (d) eddy kinetic energy (cm^2 s^{-2}).

[1991] used 10 days for the integral timescale at the thermocline level, and in the interior of the eastern North Atlantic, *Spall et al.* [1993] estimated the integral timescales at 1100 m depth to be 5–8 days for floats caught in wave-like circulations, and 13–23 days for floats that made long zonal excursions. All of these estimates are larger than the current estimated values. This is probably due to the smaller temporal and spatial scales of the variability associated with the undercurrent near the complex boundary, which is evident in the float trajectories and in the along-slope speed (Figure 7). Using only float segments east of 11°W, i.e., closer to the boundary, the average zonal and meridional integral timescales were even smaller, 2 days and 3.5 days respectively.

[36] Figure 14 shows the mean ''pseudo-Eulerian'' fields based on the float data. The degrees of freedom were estimated by determining the number of unique four-day time segments (the integral timescale) in each box and dividing by two, as also done by *Owens* [1991]. As noted above, the data are concentrated in the regions immediately south and west of the Iberian Peninsula; maximum degrees of freedom in an averaging area reached 30.

[37] The mean temperature field is shown in Figure 14b. As expected, maximum temperatures are observed along the boundary, due to the advection of the warmest, most saline MW in the boundary undercurrent. The large downstream (or along-slope) decrease in temperature north of St. Vincent's Spur indicates strong mixing there. Mean temperature along the boundary north of about 37.5°N was 11.25–11.50°C. The westward intrusion of MW west of the Iberian Peninsula is clearly evident by the relatively large, homogeneous pool with mean temperatures 11.00–11.25°C, and more specifically west of the Estremadura Promontory, where a patch with temperature greater than 11.25°C was observed. There is a relatively strong meridional temperature gradient at about 36°N. This represents the boundary between the effects of MW and cooler, fresher waters of southern origin, as also discussed in terms of the hydrographic climatology by *Iorga and Lozier* [1999a]. Interestingly, the float trajectories revealed that MW does spread into the Gulf of Cadiz (see Figure 8), but the influx of southern water into the gulf apparently helps to maintain a strong property gradient there.

[38] Mean velocity vectors are shown in Figure 14c. Vectors are displayed only if there were five or more degrees of freedom and at least two floats in the averaging area. Ellipses represent 90% confidence intervals aligned with the principle axes of variance. The advective signature of the undercurrent is apparent along the continental slope, and, as in Figures 6 and 7, there was a distinct decrease in mean speed as the undercurrent rounds Cape St. Vincent. Maximum mean velocities in the averaging areas south of the Iberian Peninsula were 0.10–0.15 m s^{-1}, while along the slope west of Iberia, mean speeds were generally 0.05–0.07 m s^{-1}. Another clear pattern is the relatively strong mean flow westward and offshore from St. Vincent's Spur to just north of Gorringe Bank, then a split, with one branch turning southwestward and the other continuing westward. Over the Tagus Abyssal Plain and in the interior Gulf of Cadiz, it is quite difficult to discern a robust pattern of the mean circulation: mean velocities are weaker and generally not significantly different from zero at the 90% confidence level. In the eastern Tagus Abyssal Plain, bounded by Gorringe Bank to the south and the Estremadura Promontory to the north, velocities are generally 0.01–0.04 m s^{-1}, and similar in the Gulf of Cadiz. There is no particularly strong pattern of anisotropy in the variability, except somewhat along the boundary, presumably due to the steering influence of the bottom slope.

[39] Maximum eddy kinetic energy (EKE) was found in the strong jet south of Portugal, where values exceeded 100 $\times 10^{-4}$ m^2 s^{-2} (Figure 14d). The next most dominant feature is the tongue of values greater than 50 $\times$ 10^{-4} m^2 s^{-2} extending northwestward from St. Vincent's Spur through the gateway, passing north of Gorringe Bank. This probably results from the occasional offshore intrusion of the undercurrent, as well as the indirect, stirring effect of meddies that form near Cape St. Vincent and translate across the Tagus Abyssal Plain. Enhanced EKE is also apparent around the Estremadura Promontory, another site of meddy formation.

[40] *Davis* [1991] discussed how Eulerian mean velocities estimated from unevenly distributed float data may be biased in the direction down the gradient of float concentration. He showed that this bias can be estimated from the eddy diffusivity and the concentration of float observations according to

$$\hat{u}_i = u_i - K_{ii}\frac{\partial \ln(C)}{\partial x_i}$$

where $\hat{u}_i$ is the measured velocity, u is the true mean, K_{ii} is the eddy diffusivity, C is the concentration of observations, taken here to be the number of degrees of freedom, and i = 1, 2 for zonal and meridional components. Diffusivity was estimated according to $K_{ii} = \langle \overline{u_i'^2} \rangle T_i$ where T is the integral timescale [*Taylor*, 1921]. The gradient of ln(C) was calculated by a least squares fit to a plane of ln(C) over a 1.5 $\times$ 1.5° (3 $\times$ 3 bins) area. The resultant bias velocity field is shown in Figure 15. The bias estimates are generally small, less than 0.02 m s^{-1}. All the bias estimates were less than the 90% confidence limits for the mean velocity, and almost all are less than the standard errors. The larger values are associated with stronger gradients in the degrees of freedom distribution. Due to their small magnitude compared to sampling errors, no correction for array bias was made to the mean velocities.

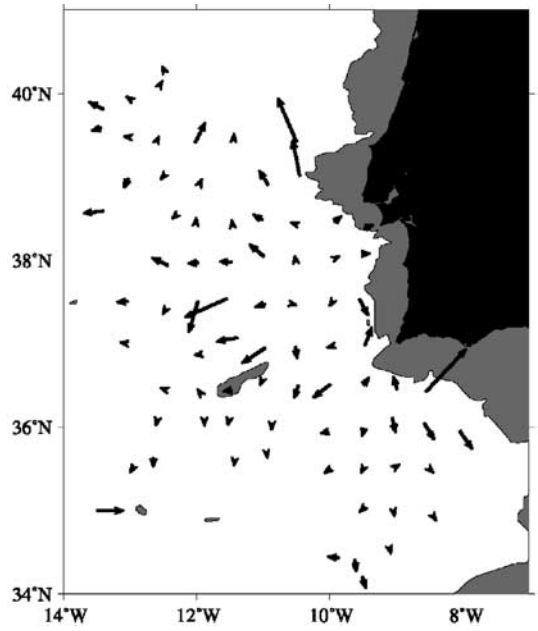

Figure 15. Array bias for mean velocity vectors shown in Figure 16c (cm s^{-1}). Note difference in velocity scale compared to Figure 14.

[41] The float data set can also be used to investigate particle dispersion and diffusivity. *LaCasce and Bower* [2000] used the AMUSE float data set, as well as three other float data sets to study relative and single-particle dispersion in the North Atlantic. They estimated the zonal and meridional diffusivities from the time rate of change of particle dispersion according to

$$K_{ii} = \frac{1}{2}\frac{d\overline{x_i'^2}}{dt}$$

using all the AMUSE trajectories, divided up into 50-day segments, and obtained a value for the total absolute diffusivity (zonal + meridional) of 3.3 ± 0.8 $\times$ 10^3 m^2 s^{-1} (error is 90% confidence limit). There was a significant meridional anisotropy, which these authors attributed to the effects of the mean flow, for which no correction was applied. These effects can even be seen qualitatively in Figure 8, which show enhanced spreading in the meridional direction due to the northward advection of floats along the western Portuguese slope.

[42] For comparison, we have estimated diffusivities based on the ideas of *Taylor* [1921], who showed that on long timescales in homogeneous, stationary turbulence, diffusivity can be expressed in terms of velocity variance and integral timescale as defined above. Here again we used only the nonmeddy observations, and the velocity residuals were estimated in the same manner as for the integral timescale, i.e., by removing the spatially dependent mean velocity field. Averaging over all the floats, the zonal and meridional velocity variances were 33 (30, 36) $\times$ 10^{-4} m^2 s^{-2} and 30 (28, 33) $\times$ 10^{-4} m^2 s^{-2}, respectively, where the numbers in parentheses represent 95% confidence limits. The degrees of freedom, ~800, were estimated from the total number of float days divided by twice the integral

timescale (4 days). These lead to estimates of the zonal and meridional diffusivities of $K_{11} = 1.1(1.0, 1.3) \times 10^3$ m^2 s^{-1} and $K_{22} = 1.0$ (0.9, 1.2) $\times 10^3$ m^2 s^{-1}. The sum, 2.1×10^3 m^2 s^{-1}, is slightly lower than the 3.3×10^3 m^2 s^{-1} estimate of *LaCasce and Bower* [2000], and there is no significant anisotropy. Both of these differences can be attributed to our removal of the spatially dependent mean flow.

4. Discussion

4.1. Transition of Mediterranean Undercurrent in the Gulf of Cadiz

[43] The high-resolution hydrographic observations described in section 3.1 above have revealed the transition of the MW outflow from a gravity current to an intermediate-depth jet. A rapid decrease in outflow salinity, temperature and density and a deepening of the outflow over a 75-km segment of the outflow path between 7°30′W and 8°10′W indicate enhanced turbulent entrainment of overlying North Atlantic Central Water occurs here, and represents the last entrainment event before the lower core of the outflow reaches neutral buoyancy as it enters Portimao Canyon. It is instructive to examine these results in the context of the one-dimensional streamtube model results for the MW outflow described by *Price and Baringer* [1994]. Their outflow simulation was initialized at the western end of the Strait of Gibraltar with observed values for salinity, temperature, density and speed, and then allowed to run into the Gulf of Cadiz using a realistic (but smoothed) bathymetry data for the gulf. As the simulated outflow leaves the strait and encounters the steeper continental slope, it accelerates and broadens, the bulk Froude number exceeds one, and intense entrainment occurs. This entrainment stops within about 50 km of the strait (before crossing 7°W) due to the loss of negative buoyancy and the turning of the outflow along the isobaths (due to Coriolis acceleration). From that point westward, the simulated outflow, in nearly geostrophic balance, gradually slides down the slope south of the Iberian Peninsula *without* further entrainment, and reaches neutral buoyancy near Cape St. Vincent. *Price and Baringer* [1994] showed that the simulation results were in general agreement with the observations available at the time.

[44] Our observations in the western gulf seem to indicate that some entrainment does take place farther downstream than indicated by the model, most likely because local bottom slopes are steeper than what was used for the simulations. Near the strait, where entrainment is strong, *Price and Baringer* [1994] report a bottom slope of 12×10^{-3}. The slope at the eastern edge of the AMUSE survey (7°30′W) (between the 1000 and 1400 m isobaths) is comparable, 10×10^{-3}, but increases eight-fold to about 80×10^{-3} in the eastern Portimao Canyon. So even though the potential density difference between the outflow and the surroundings is lower here than near the strait by about a factor of four (0.3 kg m^{-3}, Figure 4a, compared to about 1.2 kg m^{-3}), the extreme steepening apparently accelerates the flow sufficiently to cause entrainment. Without direct observations of the velocity profile, such as those available to *Price and Baringer* [1994], it is not possible to estimate Froude numbers and confirm this idea, but it is consistent with our observations. Close inspection of Figure 6 from *Price and Baringer* [1994] also supports this idea: it shows that the simulation overestimates their observations of salinity and density in the western Gulf of Cadiz, perhaps indicating there is missing entrainment in the simulation.

[45] The high-resolution hydrographic survey also revealed the existence of a core or vein of outflow water that was denser than the traditional lower core. This vein was also observed by *Ambar et al.* [2002] during 1997 in the same region. During the AMUSE survey, this denser vein detached from the seafloor just upstream (southeast) of Portimão Canyon, while the traditional lower core floated off slightly farther downstream, just as it entered the canyon. The dense vein could be traced continuously to the western limit of the survey area. *Käse and Zenk* [1996] also noted the existence of salinity maxima deeper than the traditional lower core between Portimão Canyon and Cape St. Vincent, and further pointed out the 1400-m depth of the lower salinity maximum observed in the Cadiz Meddy, found just southwest of Cape St. Vincent [*Prater and Sanford*, 1994]. They do not however discuss the density of this deep salinity maximum. In fact, the deep salinity maximum in the Cadiz Meddy has a density of about 32.3, similar to the dense vein observed during AMUSE. We propose that these deep salinity maxima do not result from a deepening of the traditional lower core MW, but rather indicate the presence of a dense core or vein of MW that is separated from the traditional lower core. This core may not always exist, but when it does, it may end up in meddies formed near this region. Its fate farther downstream is unknown.

4.2. MW Spreading Pathways

[46] The float observations have provided direct information on the spreading pathways of MW from the Gulf of Cadiz into the ocean interior that can be compared to results from similar studies that were based mainly on hydrographic distributions. From a set of hydrographic sections around the southwestern Iberian Peninsula, *Zenk and Armi* [1990] concluded that the lower core of the Mediterranean outflow flows mainly through the ''gateway'' between Cape St. Vincent and Gorringe Bank, then ''splits,'' with the major branch veering offshore toward the west and northwest, and a minor branch continuing along the boundary northward. From a different set of hydrographic sections, *Daniault et al.* [1994] illustrate a similar pattern, with the added detail of a cyclonic turning of the offshore branch northwest of Gorringe Bank. Using historical data from the US, former USSR and other selected cruises, *Shapiro and Meschanov* [1996] also proposed that the main spreading pathway was through the gateway and then offshore toward the northwest. They also found evidence of branches directed southwestward from Cape St. Vincent, passing south of Gorringe Bank. However, they did not show the vein directed northward along the slope.

[47] The most recent, and perhaps most comprehensive of these hydrography-based studies is that of *Iorga and Lozier* [1999a], who used the new North Atlantic climatology [*Lozier et al.*, 1995] to identify the MW spreading pathways. Their composite summary (their Plate 2, reproduced here in Figure 16) has a number of features that are consistent with the float observations. In particular, they identify the three main MW spreading pathways indicated

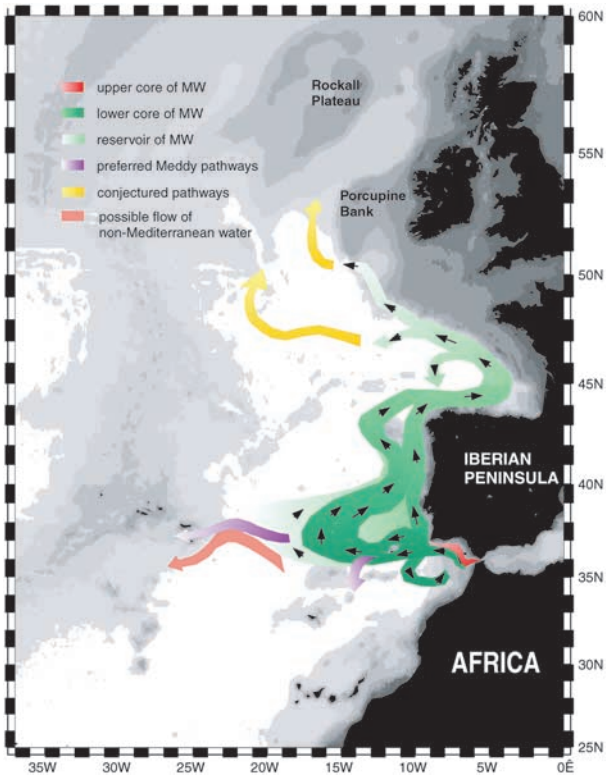

Figure 16. Composite summary of MW spreading pathways from *Iorga and Lozier* [1999a]. Reprinted with permission.

by the floats that were shown in Figure 9: one branch recirculating cyclonically in the Gulf of Cadiz, a second branch directly westward from Cape St. Vincent, and a third northward along the western Portuguese slope. Although it is not shown in Figure 9a (Gulf of Cadiz path), three floats made complete cyclonic circuits around the Gulf of Cadiz and back into the undercurrent, consistent with the closed circulation indicated in Figure 16 (see also Figure 8f). On the other hand, the float and hydrography-based interpretations differ west of Portugal, over the Tagus Abyssal Plain. The floats indicate that much of the northward branch along the western Portuguese slope turns offshore and veers cyclonically from the southern flank of the Estremadura Promontory into the Tagus Abyssal Plain (Figures 8 and 9c). The hydrography-based picture shows the northward path along the boundary continuing northward around the promontory and merging with a branch that makes an anticyclonic loop over the plain. There are several possible explanations for this apparent discrepancy. First, the Iorga and Lozier picture represents MW pathways at all levels, and others have shown that the upper core remains tighter to the slope west of Portugal compared to the lower core [*Zenk and Armi*, 1990]. So the northward penetration of the northward branch may be more representative of the upper core. Second, some of the sweeping anticyclonic branch over the Tagus Abyssal Plain is beyond the region of most float observations, and thus may be missing in the float-based picture. Third, the amount of float data over the plain in general may be insufficient. Whereas the anticyclonic circulation is not evident in the mean fields derived from the floats, individual float tracks (not shown) reveal both northward and southward flow over the plain. More direct velocity observations are needed to resolve this.

[48] Several investigators have attempted to quantify the transports through this region from geostrophic calculations. One of the most detailed was *Mazé et al.* [1997], who used 53 hydrographic stations collected around the southwestern Iberian Peninsula in May 1989 (Bord-Est 3 Experiment) to infer the volume transport in six layers through the water column. Two of their results were unexpected and are worth comparing with the float mean velocities (Figure 14c).

[49] First, they found 10.6 Sv of northward transport across 37°N adjacent to the eastern boundary at the Mediterranean Water level. As the authors admit, this value is high compared to estimates of the transport exiting the Gulf of Cadiz at the MW level. They attribute their high value to 1) a different reference level choice compared to earlier estimates, and 2) the contribution of transport from south of the Gulf of Cadiz. In Figure 17a we show the mean meridional velocity at 37 N from the float data (extracted from Figure 14c, but including all area averages, not just those with >5 degrees of freedom and >2 floats) as a function of longitude. The change in sign of v along 37 N, northward adjacent to the boundary switching to southward west of about 11°W was also seen by *Mazé et al.* [1997] (although most velocity estimates here were not significantly different from zero at the 90% confidence level). This gives the distinct impression of the flow turning cyclonically around the northern and western flanks of Gorringe Bank, as also indicated by *Daniault et al.* [1994]. The 10.6 Sv implies a zonally and vertically averaged northward velocity of 0.07 m s^{-1} over their 1000-m thick MW layer (includes both upper and lower core layers) over a 150 km wide current (9°W–10.75°W, see their Figure 12). From the float data, the peak mean northward velocity is about 0.07 cm s^{-1}, at about 9.5°W, and the neighboring values are half that or less. It seems

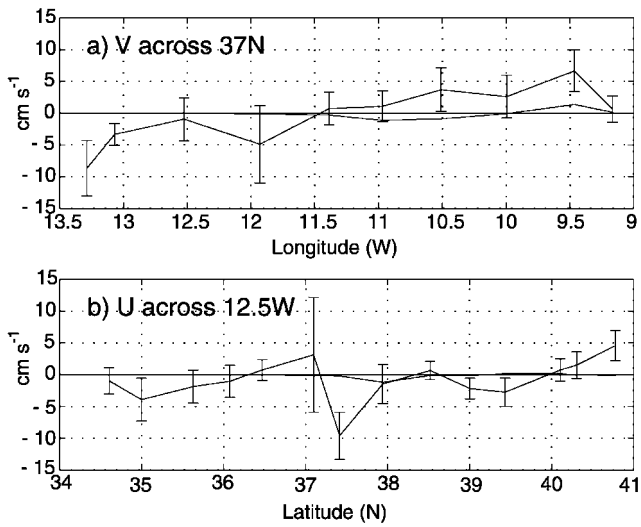

Figure 17. (a) Mean meridional velocity across 37°N as a function of longitude, extracted from Figure 14c. Error bars indicate 90% confidence intervals, and other thin line shows array bias from Figure 15. (b) Same as (a) but showing zonal velocity across 12.5°W as a function of latitude.

unlikely that significantly higher mean velocities are present above or below our MW layer (950–1250 dbar), at least not high enough to give 10.6 Sv northward, The more likely explanation is that the high transport observed by *Mazé et al.* [1997] was a transient event. If we take the average northward speed from Figure 17a (0.026 m s^{-1}) and apply it to the zonal extent of the northward flow and over a 1000-m thick layer, the result is 6.8 Sv.

[50] *Mazé et al.* [1997] also found weak *eastward* transport across the meridian 12.5°W (between 38 and 43°N) at the MW level during their survey. From this result, they argued that the *westward* salt flux at the MW level is accomplished entirely via meddies and other eddies and not by large-scale advection. Figure 17b shows the mean zonal velocity across 12.5W from the float data. The mean over the entire section is weak westward, -0.008 m s^{-1}, but in light of the 90% confidence limits, which are at least ± 0.02 m s^{-1} for almost all the box averages, we conclude that the mean zonal velocity across this meridian is not statistically different from zero.

5. Summary

[51] Float and hydrographic observations from around the southwestern Iberian Peninsula have been examined to investigate the pathways, rates and mechanisms of MW spreading from the Gulf of Cadiz into the ocean interior. A high-resolution hydrographic survey south of Portugal reveals in detail the evolution of the Mediterranean Undercurrent from a bottom-intensified density current to an intermediate-depth jet. The properties of the outflow change dramatically due to turbulent entrainment as the outflow approaches Portimão Canyon, a major topographic feature of the slope south of Portugal. The traditional lower salinity core reaches approximate neutral buoyancy as it enters Portimão Canyon, and θ-S changes downstream from that location are much more gradual. We suggest that the extreme (∼eight-fold) increase in the bottom slope approaching Portimao Canyon leads to an acceleration of the gravity current enough to initiate entrainment, leading to decreases in salinity and density and a neutrally buoyant outflow. In recent simulations of this outflow by *Price and Baringer* [1994], entrainment was not apparent in this location due to the smoothed, less steep topography used in the simulation.

[52] A continuous vein of MW denser than the traditional lower core could be traced from upstream of Portimão Canyon to the western edge of the survey, 9°W. In some locations, it was split away from the traditional lower core by submarine headlands. We have argued that previous observations of salinity maxima deeper than the traditional lower core were not due to a simple deepening of that core, but rather originate from denser MW in the Gulf of Cadiz. Geostrophic velocity calculations reveal a narrow (∼10-km wide) synoptic undercurrent with peak downstream speeds of about 0.4 m s^{-1} during the hydrographic survey.

[53] The direct float velocity observations reveal a dramatic decrease in the strength of the Mediterranean Undercurrent from upstream to downstream of Cape St. Vincent: float speeds greater than 0.2 m s^{-1} were common upstream, and rare downstream. The cross-stream structure of velocity also changes dramatically around Cape St. Vincent. South of Portugal, a strong, jet-like structure emerges from the float data, with peak mean speed of 0.2 m s^{-1}, and a cyclonic shear zone about 30 km wide. The inshore, anticyclonic shear zone could not be resolved in the mean. West of Portugal, a broader, weakly sheared northward mean flow of about 0.06 m s^{-1} and about 50 km wide was found. These along-stream changes in undercurrent speed and structure are attributed mainly to the broadening and flattening of the continental slope along the western Portuguese coast between Cape St. Vincent and Lisbon/Setubal Canyons. This is further supported by the observations of accelerated flow farther north, along the southern flank of the Estremadura Promontory, where the bottom slope again becomes steep. Also striking in these observations was the extreme variability, indicated by frequent flow reversals and standard deviations of about 0.1 m s^{-1}.

[54] The trajectories of all the AMUSE floats at the lower core level (meddy and nonmeddy) directly illustrate the predominant MW spreading pathways from the undercurrent south of Portugal, namely, southward into the interior Gulf of Cadiz, west–northwestward from Cape St. Vincent into the interior, and northward along the western Portuguese slope. Most of the floats (60%) passed through the gateway between Cape St. Vincent and Gorringe Bank, then left the continental slope between Cape St. Vincent and the Estremadura Promontory, while 30% entered the Gulf of Cadiz. Only 10% made it north of the Estremadura Promontory. This is consistent with previous interpretations of large-scale hydrographic distributions, which show the most saline water spreading westward from the western Portuguese slope.

[55] The float tracks reveal not only where MW leaves the boundary, but also the mechanism. When meddies are forming along the slope, they temporarily block the undercurrent and divert MW *not* in meddies into deep water. Once the meddy moves away, the flow resumes along the boundary. On average, the MW in the lower core spreads rapidly westward at first, then more slowly toward the west–northwest into the southern Tagus Abyssal Plain. Spreading rates averaged over more than six months are 0.01–0.02 m s^{-1}.

[56] All the nonmeddy, lower core float observations were averaged in $0.5 \times 0.5°$ areas to reveal the spatial patterns of mean temperature, velocity and eddy kinetic energy for the background field. Integral timescales in the study area were about 4 days, smaller than estimates farther offshore in the eastern Atlantic and in the western Atlantic, presumably due to the smaller space-timescales of the variability, induced by flow over complex topography. Both mean temperature and mean velocity show sharp decreases in the undercurrent from upstream to downstream of Cape St. Vincent. Advective pathways are indicated following the boundary and shooting offshore from St. Vincent's Spur. EKE is elevated in the undercurrent south of Portugal, where values exceed 100×10^{-4} m^2 s^{-2}, and a well-defined tongue of high EKE ($>50 \times 10^{-4}$ m^2 s^{-2}) extends west–northwestward from the spur, possibly reflecting the variability in the offshore branch and the stirring effect of newly formed meddies.

[57] The direct pathway observations support many of the MW spreading features revealed in detailed studies of the hydrographic fields in this region, for example that of *Iorga*

and Lozier [1999a]. The common features include cyclonic recirculation south of the undercurrent in the Gulf of Cadiz and branching from St. Vincent's Spur into northward and westward veins. One discrepancy occurs over the Tagus Abyssal Plain, where the hydrography indicates the main part of the westward branch turns northward, then northeastward back toward the boundary and joins with the northward branch. Most, although not all of the floats indicate the northward branch separating from the boundary near the Estremadura Promontory and turning southwestward, in opposition to the hydrography-based scheme. This difference remains to be resolved. The mean float velocities suggest a lower northward transport across 37°N at the MW level (~7 Sv) compared to ~11 Sv reported by *Mazé et al.* [1997], which may be an overestimate caused by transient features. The float observations do however agree with their conclusion that there is no large-scale advection of MW across 12.5°W in the Iberian Basin, and that the westward salt flux must be accomplished by meddies and other eddies.

[58] A number of questions remain to be addressed regarding the spreading of MW in the eastern North Atlantic. In particular, the details of the meddy formation process are still unknown, and new observations are needed to understand it better. This will be very challenging in light of the intermittent nature of the formation process, the lack of a reliable surface signature, and its small spatial scale. As part of such a study, one would hope to learn why some MW becomes trapped in the meddy while other MW is diverted offshore by the meddy, as observed with the floats. The relative importance of meddies and nonmeddy spreading processes to the maintenance of the Mediterranean salt tongue is another aspect of fundamental importance that is still not well understood.

[59] **Acknowledgments.** AB gratefully acknowledges J. LaCasce and S. Lozier for enlightening discussions that helped in the interpretation of the observations. We also thank H. Hunt Furey for assistance with preparing the final figures. W. Zenk kindly allowed us to include the IfM data in our analysis. L. Armi is acknowledged for his role in collecting the AMUSE observations. The comments of two anonymous reviewers helped to improve this manuscript. This work was supported by the U.S. National Science Foundation (Grant No. OCE-9616952 and Grant No. OCE-9531877) to the Woods Hole Oceanographic Institution. Funding from the Fundação Portuguesa para a Ciência e Tecnologia (Grant BD/19535/99) to NS is also acknowledged. This is Woods Hole Oceanographic Institution Contribution Number 10480.

References

Ambar, I., A shallow core of Mediterranean Water off western Portugal, *Deep Sea Res., Part I*, *30*, 677–680, 1983.

Ambar, I., and M. R. Howe, Observations of the Mediterranean outflow, 1, Mixing in the Mediterranean outflow, *Deep Sea Res., Part I*, *26*, 535–554, 1979a.

Ambar, I., and M. R. Howe, Observations of the Mediterranean outflow, 2, The deep circulation in the vicinity of the Gulf of Cadiz, *Deep Sea Res., Part I*, *26*, 555–568, 1979b.

Ambar, I., L. Armi, A. Bower, and T. Ferreira, Some aspects of time variability of the Mediterranean Water off south Portugal, *Deep Sea Res., Part I*, *46*, 1109–1136, 1999.

Ambar, I., N. Serra, M. J. Brogueira, G. Cabeçadas, F. Abrantes, P. Freitas, C. Gonçalves, and N. Gonzalez, Physical, chemical and sedimentological aspects of the Mediterranean Outflow off Iberia, *Deep Sea Res., Part II*, *49*, 4163–4177, 2002.

Armi, L., and W. Zenk, Large lenses of highly saline Mediterranean Water, *J. Phys. Oceanogr.*, *14*, 1560–1576, 1984.

Baringer, M. O., and J. F. Price, Mixing and spreading of the Mediterranean outflow, *J. Phys. Oceanogr.*, *27*, 1654–1677, 1997.

Bower, A. S., L. Armi, and I. Ambar, Lagrangian observations of Meddy formation during a Mediterranean undercurrent seeding experiment, *J. Phys. Oceanogr.*, *27*, 2545–2575, 1997a.

Bower, A. S., J. Pallant, and C. L. Chandler, A Mediterranean Undercurrent Seeding Experiment (AMUSE), 1, Program description and hydrographic measurements, *Woods Hole Oceanogr. Inst. Tech. Memo. WHOI-01-97*, 14 pp., Woods Hole Oceanogr. Inst., Woods Hole, Mass., 1997b.

Chérubin, L., X. Carton, J. Paillet, Y. Morel, and A. Serpette, Instability of the Mediterranean water undercurrents southwest of Portugal: Effects of baroclinicity and of topography, *Oceanol. Acta*, *23*, 551–573, 2000.

Daniault, N., J. P. Mazé, and M. Arhan, Circulation and mixing of Mediterranean Water west of the Iberian Peninsula, *Deep Sea Res., Part I*, *41*, 1614–1685, 1994.

D'Asaro, E. A., Generation of submesoscale vortices: A new mechanism, *J. Geophys. Res.*, *93*, 6685–6693, 1988.

Davis, R. E., Lagrangian ocean studies, *Annu. Rev. Fluid Mech.*, *23*, 43–64, 1991.

Davis, R. E., Preliminary results from directly measuring middepth circulation in the tropical and South Pacific, *J. Geophys. Res.*, *103*(C11), 24,619–24,639, 1998.

Heezen, B. C., and G. L. Johnson, Mediterranean under-current and microphysiography west of Gibraltar, *Bull. Inst. Oceanogr. Monaco*, *67*(1382), 1–97, 1969.

Hunt, H. D., C. M. Wooding, C. L. Chandler, and A. S. Bower, A Mediterranean Undercurrent Seeding Experiment (AMUSE), 2, RAFOS float data report May 1993–March 1995, *Woods Hole Oceanogr. Inst. Tech. Rep. WHOI-98-14*, Woods Hole Oceanogr. Inst., Woods Hole, Mass., 1998.

Iorga, M. C., and M. S. Lozier, Signatures of the Mediterranean outflow from a North Atlantic climatology, 1, Salinity and density fields, *J. Geophys. Res.*, *104*(C11), 25,985–26,009, 1999a.

Iorga, M. C., and M. S. Lozier, Signatures of the Mediterranean outflow from a North Atlantic climatology, 2, Diagnostic velocity fields, *J. Geophys. Res.*, *104*(C11), 26,011–26,029, 1999b.

Käse, R. H., and W. Zenk, Structure of the Mediterranean Water and Meddy characteristics in the northeastern Atlantic, in *Warmwatersphere of the North Atlantic Ocean*, edited by W. Krauss, pp. 365–395, Gebrüder Borntraeger, Berlin, 1996.

LaCasce, J., and A. Bower, Relative dispersion in the subsurface North Atlantic, *Journal of Marine Research*, *58*, 863–894, 2000.

Lozier, M. S., W. B. Owens, and R. G. Curry, The climatology of the North Atlantic, *Progress in Oceanography*, *36*, 1–44, 1995.

Madelain, F., Influence de la topographie du fond sur l'écoulement méditerranéen entre le Détroit de Gibraltar et le Cap Saint-Vincent, *Cahiers Océanographie*, *22*, 43–61, 1970.

Mazé, J. P., M. Arhan, and H. Mercier, Volume budget of the eastern boundary layer off the Iberian Peninsula, *Deep-Search Research I*, *44*, 1543–1574, 1997.

McDowell, S. E., and H. T. Rossby, Mediterranean water: An intense mesoscale eddy off the Bahamas, *Science*, *202*, 1085–1087, 1978.

Needler, G. T., and R. A. Heath, Diffusion coefficients calculated from the Mediterranean salinity anomaly in the North Atlantic Ocean, *J. Phys. Oceanogr.*, *5*, 173–182, 1975.

Ochoa, J., and N. A. Bray, Water mass exchange in the Gulf of Cadiz, *Deep Sea Res., Part I*, *38*, 465–503, 1991.

Oliveira, P. B., N. Serra, A. F. G. Fiúza, and I. Ambar, A study of meddies using simultaneous *in situ* and satellite observations, in *Satellites, Oceanography and Society*, *Oceanogr. Ser. 63*, edited by D. Halpern, pp. 125–148, Elsevier Sci., New York, 2000.

Owens, W. B., A statistical description of the mean circulation and eddy variability in the northwestern Atlantic using SOFAR floats, *Progress in Oceanography*, *28*, 257–303, 1991.

Prater, M. D., and T. B. Sanford, A Meddy off Cape St. Vincent, 1, Description, *J. Phys. Oceanogr.*, *24*, 1572–1586, 1994.

Price, J. F., and M. O. Baringer, Outflows and deep water production by marginal seas, *Prog. Oceanogr.*, *33*, 161–200, 1994.

Reid, J. L., On the total geostrophic circulation of the North Atlantic Ocean: Flow patterns, tracers and transports, *Progress in Oceanography*, *33*, 1–92, 1994.

Richardson, P. L., and K. Mooney, The Mediterranean outflow—A simple advection diffusion model, *J. Phys. Oceanogr.*, *5*, 476–482, 1975.

Richardson, P. L., D. Walsh, L. Armi, M. Schroder, and J. F. Price, Tracking three meddies with SOFAR floats, *J. Phys. Oceanogr.*, *19*, 371–383, 1989.

Richardson, P. L., A. Bower, and W. Zenk, A census of meddies tracked by floats, *Progress in Oceanography*, *45*, 209–250, 2000.

Serra, N., and I. Ambar, Eddy generation in the Mediterranean undercurrent, *Deep Sea Res., Part II*, *49*, 4225–4243, 2002.

Serra, N., S. Sadoux, I. Ambar, and D. Renouard, Observations and laboratory modeling of meddy generation at Cape St. Vincent, *J. Phys. Oceanogr.*, *32*, 3–25, 2002.

Shapiro, G. I., and S. L. Meschanov, Spreading pattern and mesoscale structure of Mediterranean outflow in the Iberian Basin estimated from historical data, *Journal of Marine Systems*, *7*, 337–348, 1996.

Spall, M. A., P. L. Richardson, and J. Price, Advection and eddy mixing in the Mediterranean salt tongue, *J. Mar. Res.*, *51*, 797–818, 1993.

Sparrow, M., O. Boebel, V. Zervakiz, W. Zenk, A. Cantos-Figuerola, and W. J. Gould, Two circulation regimes of the Mediterranean outflow revealed by Lagrangian measurements, *J. Phys. Oceanogr.*, *32*, 1322–1330, 2002.

Taylor, G. I., Diffusion by continuous movements, *Proc. Lond. Math. Soc.*, *20*, 196–212, 1921.

Zenk, W., On the origin of intermediate double maxima in T/S profiles from the North Atlantic, *Meteor Forschungsergeb.*, *A16*, 35–43, 1975.

Zenk, W., and L. Armi, The complex spreading pattern of Mediterranean Water off the Portuguese continental slope, *Deep Sea Res.*, *37*, 1805–1823, 1990.

A. S. Bower, Department of Physical Oceanography, Woods Hole Oceanographic Institution, Mail Stop 21, 360 Woods Hole Road, Woods Hole, MA 02543 USA. (abower@whoi.edu)

I. Ambar and N. Serra, Instituto de Oceanografia, University of Lisbon, Portugal.